# Green Fluorescent Protein (GFP): Applications, Structure, and Related Photophysical Behavior

Marc Zimmer*

*Department of Chemistry, Connecticut College, New London, Connecticut 06320*

*Received June 21, 2001*

## *Contents*



## *I. Introduction*

In the last 10 years green fluorescent protein (GFP) has changed from a nearly unknown protein to a commonly used tool in molecular biology, medicine, and cell biology. GFP is used as a biological marker. It is particularly useful due to its stability and the fact that its chromophore is formed in an autocatalytic cyclization that does not require a cofactor. This has enabled researchers to use GFP in living systems, and it has led to GFP's widespread use in cell dynamics and development studies. Furthermore, it appears that fusion of GFP to a protein does not alter the function or location of the protein. A literature search for references with GFP in the title and/or abstract for 1994 found 10 publications, while an identical search found 106 publications in February 2001. [All references to *G*ender *F*ree *P*ronouns and *G*esellschaft Fuer *F*leischfressende *P*flanzen were not counted.] Over 6000 articles using "GFP" or "Green Fluorescent Protein" in the title or abstract are indexed in Pubmed. Several reviews have recently been written about GFP[1−5] and about its applications in plants,[6] structure, dynamics,[7] reporter gene technology,[8] cell biology,[9] and in drug discovery;[10] a book has been published,[11] a volume of *Methods in Enzymology*[12] and *Methods in Cell Biology*[13] have been devoted to GFP, two CD-ROMs with images of GFP applications have been released,[14,15] and *Trends in Cell Biology* has started a series of review articles

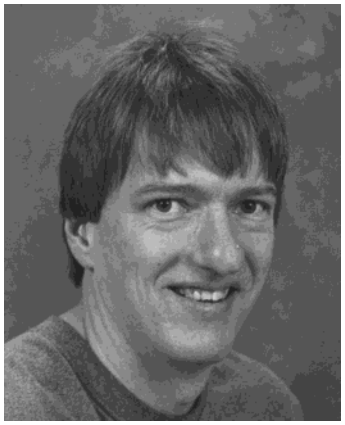

Marc Zimmer was born in Sasolburg, South Africa. He received his B.Sc. and M.Sc degrees from the University of Witwatersrand, where he worked with Professor R. Hancock. In 1988 he received his Ph.D. degree in Macrocyclic Chemistry under the supervision of Professor N. Kildahl at W.P.I. After an 18-month postdoctoral fellowship with Professor R. Crabtree at Yale University, he got a tenure track position at Connecticut College. Marc is a Henry Dreyfus Teacher−Scholar, father of two children, and Program Chair of the Inorganic Division of the American Chemical Society. He and his undergraduate students use computational methods to examine interesting systems such as green fluorescent protein, luciferase, methyl co-enzyme M reductase, histidine ammonia lyase, and urease.

* To whom correspondence should be addressed. E-mail: mzim@conncoll.edu.

10.1021/cr010142r CCC: $39.75 
Published on Web 02/02/2002

on the uses of GFP. Due to the tremendous amount of literature devoted to green fluorescent protein and its applications, this review must by necessity be selective. In this review an attempt has been made to have a comprehensive review of the chemistry of green fluorescent protein. Although applications of GFP in molecular biology, environmental studies, and medicine are reviewed, this paper is by no means a complete review of the many uses of GFP.

## II. Historical Perspective

Pliny the elder described bioluminescence as early as the first century AD.[16] Bioluminescence is the process by which visible light is emitted by an organism as a result of a chemical reaction. The reaction involves the oxidation of a substrate (called the luciferin) by an enzyme (the luciferase). Oxygen is usually the oxidant. Bioluminescent organisms are found in a variety of environments. Common examples are insects, fish, squid, sea cacti, sea pansies, clam, shrimp, and jellyfish. The bioluminescent systems in these organisms are not all evolutionarily conserved, and the genes coding for the proteins involved in bioluminescence are not homologous.[17] The emitted light commonly has one of three functions: defense, offense, and communication.

Green fluorescent proteins are found in numerous organisms; however; in this review, GFP and green fluorescent protein refer exclusively to the GFP found in the jellyfish *Aequorea aequorea* (also commonly referred to as *Aequorea victoria* and *Aequorea forskalea*[18]). This is because the *Aequorea* GFP was the first GFP for which the gene was cloned[19] and expressed,[20] and it is the GFP used in most of the tracer studies.

In 1955 it was first reported that *Aequorea* fluoresced green when irradiated with ultraviolet light.[21] Two proteins in *Aequorea* are involved in its bioluminescence, aequorin and green fluorescent protein. Aequorin (the luciferase) contains coelenterazine (the luciferin). Upon binding three calcium ions the aequorin oxidizes the coelenterazine with a protein-bound oxygen resulting in a $Ca_3$-apo-aequorin-coelenteramide complex which in vitro emits blue light.[18,22,23] However, *Aequorea* does not emit blue bioluminescence; instead, the aequorin complex undergoes radiationless energy transfer to GFP which gives off green fluorescence,[5,24,25] see Figure 1. No binding between aequorin and GFP is observed in solution.[26] In vitro energy transfer can be obtained by coadsorption of aequorin and GFP on DEAE cellulose membranes.[26] The crystal structure of aequorin was recently solved.[27]

Shimomura isolated a small peptide fragment containing the chromophore from a papain digest of heat-denatured GFP. By synthesizing small model compounds and comparing them to the chromophore of GFP, he deduced the structure of the chromophore in 1979.[18,28] The 4-(*p*-hydroxybenzylidene)imidazolid-5-one structure he proposed is shown in Figure 2.

Later studies confirmed the structure of the chromophore and showed that the chromophore containing peptide fragment is a cyclized hexapeptide formed from residues Phe64-Ser-Tyr-Gly-Val-Gln69 of GFP,[29]

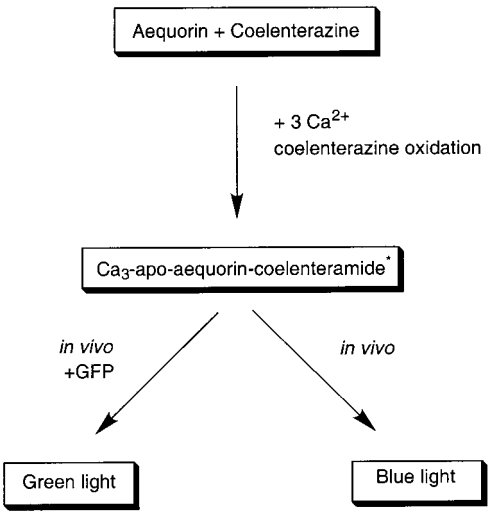


**Figure 1.** Bioluminescence in *Aequorea victorea*. Upon binding three calcium ions the aequorin oxidizes the coelenterazine with a protein-bound oxygen resulting in a $Ca_3$-apo-aequorin-coelenteramide complex, which in vitro emits blue light. In vivo the aequorin complex undergoes radiationless energy transfer to GFP, which gives off green fluorescence.

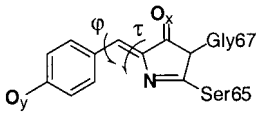


**Figure 2.** 4-(*p*-Hydroxybenzylidene)-imidazolid-5-one structure of the chromophore. The $O_y$, $O_x$, and N atoms shown in bold are possible protonation sites. The $\varphi$ and $\tau$ dihedral angles can rotate in the excited state.

see section V. The sequence of wild-type GFP was first determined in 1992[19] and is given in Table 1. It contains a trivial Q80R mutation that is present in most cDNA constructs derived from the original sequence. In 1994 GFP was expressed and it was found that the resultant protein fluoresced green,[20] proving that the chromophore was formed by an intramolecular autocatalytic cyclization.

## III. Crystal Structures of GFP–Light in a Can

The Protein Data Bank currently lists 22 GFP and GFP mutant crystal structures as well as crystal structures of 2 GFP analogues, see Table 2. GFP analogues from corals, sea pens, sea squirts, and sea anemones have been isolated in a variety of fluorescent and nonfluorescent colors. They all have similar structures to *aequorea* GFP and are discussed in more detail in section VIII. In this section of the review the common features of all the *aequorea* GFP structures are discussed.

Even though many of the mutants have very different spectral properties, their structural features are remarkably similar. The structures of the wild-type[30] and S65T mutant GFP[31] were the first to be solved. Although wild-type GFP and most subsequent GFP mutants were crystallized as dimers, some structures of monomeric GFP have been solved. GFP is not an obligate dimer, and dimer formation is very dependent on the crystal growth conditions.[7] GFP has a unique 11 $\beta$-sheet barrel-like structure with a

**Table 1. GFP Nucleotide Sequence of Wild-Type *Aequorea* and Amino Acid Sequence of Wild-Type *Aequorea***

a. GFP nucleotide sequence of wild-type *Aequorea*

```
1   tacacacgaa taaaagataa caaagatgag taaaggagaa gaacttttca ctggagttgt
61  cccaattctt gttgaattag atggtgatgt taatgggcac aaattttctg tcagtggaga
121 gggtgaaggt gatgcaacat acggaaaact tacccttaaa tttatttgca ctactggaaa
181 actacctgtt ccatggccaa cacttgtcac tactttctct tatggtgttc aatgcttttc
241 aagataccca gatcatatga aacagcatga ctttttcaag agtgccatgc ccgaaggtta
301 tgtacaggaa agaactatat ttttcaaaga tgacgggaac tacaagacac gtgctgaagt
361 caagtttgaa ggtgataccc ttgttaatag aatcgagtta aaaggtattg attttaaaga
421 agatggaaac attcttggac acaaattgga atacaactat aactcacaca atgtatacat
481 catggcagac aaacaaaaga atggaatcaa agttaacttc aaaattagac acaacattga
541 agatggaagc gttcaactag cagaccatta tcaacaaaat actccaattg gcgatggccc
601 tgtccttta ccagacaacc attacctgtc cacacaatct gccctttcga aagatcccaa
661 cgaaaagaga gaccacatgg tccttcttga gtttgtaaca gctgctggga ttacacatgg
721 catggatgaa ctatacaaat aaatgtccag acttccaatt gacactaaag tgtccgaaca
781 attactaaaa tctcagggtt cctggttaaa ttcaggctga gatattattt atatatttat
841 agattcatta aaattgtatg aataatttat tgatgttatt gatagaggtt attttcttat
901 taaacaggct acttggagtg tattcttaat tctatattaa ttacaatttg atttgacttg
961 ctcaaa
```

b. amino acid sequence of wild-type *Aequorea*

```
MSKGEELFTGVVPILVELDGDVNGHKFSVSGEGEGDATYGKLTLKFICTTGKLPVPWPTL
VTTFSYGVQCFSRYPDHMKRHDFFKSAMPEGYVQERTIFFKDDGNYKTRAEVKFEGDTLV
NRIELKGIDFKEDGNILGHKLEYNYNSHNVYIMADKQKNGIKVNFKIRHNIEDGSVQLAD
HYQQNTPIGDGPVLLPDNHYLSTQSALSKDPNEKRDHMVLLEFVTAAGITHGMDELYK
```

**Table 2. Description of All the Crystal Structures of Green Fluorescent Protein, Its Mutants, and Homologs in the Protein Databank[256]**

| PDB code | description | ref |
|---|---|---|
| 1GFL | wild-type (Q80R), dimer | 30 |
| 1EMA | S65T | 31 |
| 1BFP | Y66H, Y145H, blue mutant | 84 |
| 1EMB | Wild-type (Q80R), monomer | 36 |
| 1EML | F64L, I167T, K238N, dimer (monoclinic) | 59 |
| 1EMC | F64L, I167T, K238N, dimer (monoclinic) | 59 |
| 1EME | F64L, I167T, K238N, dimer (cubic) | 59 |
| 1EMF | F64L, Y66H, V163A,blue mutant, dimer (cubic) | 59 |
| 2EMO | F64L, Y66H, V163A, blue mutant, dimer (cubic) | 59 |
| 1EMK | F64L, S65C, I167T, K238N, dimer | 59 |
| 1EMM | F64L, dimer | 59 |
| 2EMD | F64L, Y66H, blue mutant, dimer (cubic) | 59 |
| 2EMN | F64L, Y66H, blue mutant, dimer (hexagonal) | 59 |
| 1YFP | S65G, V68L, S72A, Q80R, T203Y, yellow mutant | 116 |
| 2YFP | S65G, V68L, S72A, Q80R, H148G, T203Y, yellow mutant | 116 |
| 1C4F | S65T at pH 4.6 | 86 |
| 1EMG | S65T at pH 8.0 | 86 |
| 1B9C | F99S, M153T, V163A a folding mutant, dimer | 58 |
| 1F09 | S65G, V68L, S72A, Q80R, H148Q, T203Y, yellow mutant with two bound iodides | 206 |
| 1F0B | S65G, V68L, S72A, Q80R, H148Q, T203Y, yellow mutant | 206 |
| 1H6R | C48V, S65A, V68L, S72A, Q80R, N149C, M153V, S202C, T203Y, D234H, oxidized state | 257 |
| 1HUY | S65G, V68L, Q69M, S72A, T203YCitrine, an improved yellow mutant | 258 |
| 1G7K | DsRed | 248 |
| 1GGX | DsRed | 247 |

diameter of about 24 Å and a height of 42 Å. The $\beta$-sheets form the walls of a can, and an α helix runs diagonally through the can. The chromophore is in the center of the 11 $\beta$-sheets and is linked by the α-helical stretch that runs through the center of the barrel, see Figure 3.

There is only one obvious irregularity in the $\beta$ barrel, between strands 7 and 8.[7] Short α-helical sections form lids on both ends of the $\beta$-can. The chromophore has a cis geometry as shown in Figure 2 and is well protected in the center of the barrel. By enclosing the chromophore in the can, it may be protected from quenching by oxygen[32] and attack by hydronium ions.[33] Deletion mapping experiments have shown that nearly the entire structure (residues 2−232[34] or 7−229[35]) is required for chromophore formation and/or fluorescence. Several polar residues and water molecules comprise a hydrogen-bonding network around the chromophore. Figure 4 shows all the short-range interactions between the chromophore and the surrounding protein in wild-type and S65T GFP.

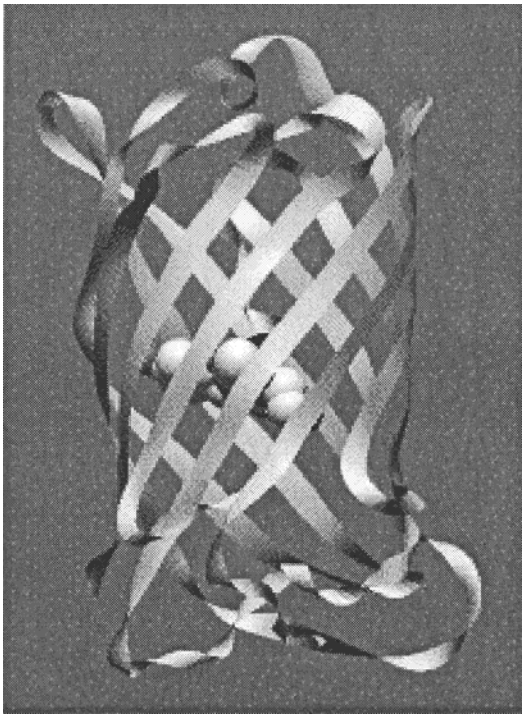

**Figure 3.** Solid-state structure of GFP. The chromophore is located in the center of the 11-sheet $\beta$-barrel and is shown with a CPK representation. (Coordinates for the figure were obtained from the PDB, code 1GFL).

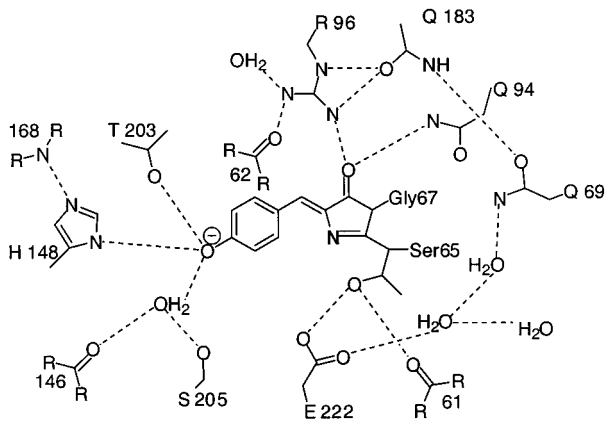


**Figure 4.** Schematic diagram of the interactions between the chromophore and its surroundings in the S65T[31] mutant. Possible hydrogen bonds are drawn as dashed lines.

Both the protonation state of the chromophore and its surrounding as well as the hydrogen-bonding network around the chromophore play an important role in the photophysics of GFP and are discussed in section VI. A large cavity that occupies a volume of ~135 Å$^3$ is found on one side of the chromophore.[31] The cavity is lined by Leu42, Ser65, Tyr66, Val68, Gln69, Leu201, Thr203, Glu222, and Val224, does not open to bulk solvent, and contains four water molecules in 1EMA.

Little is known about the interaction between GFP and aequorin. It has been suggested that an area of negative potential on GFP[36] or a hydrophobic patch which includes residues 206, 221, and 223[37] could be the binding site.

## IV. Folding and Thermosensitivity

Folding of GFP into the 11-strand $\beta$-barrel shown in Figure 3 is most likely crucial to the formation of the chromophore and its bioluminscene. Early research on GFP and the crystal structures of GFP have shown that the chromophore is formed by an intramolecular cyclization of 65Ser-Tyr-Gly67. Formation is autocatalytic, and the only external requirement is the presence of oxygen.[20,38] One can therefore assume that it is the protein sequence and its resultant three-dimensional structure that is responsible for setting up the intramolecular cyclization between residues 65 and 67 of GFP. This assumption has been confirmed by the total chemical synthesis of a precursor molecule of *Aequorea* green fluorescent protein, which when deprotected and subjected to refolding conditions formed GFP with identical spectroscopic properties to native GFP.[39] The $\beta$-can structure protects the chromophore and is presumably responsible for GFP's stability.[32,33] GFP can be reversibly denatured.[33] Fluorescence is completely lost in the denatured GFP[40] but is regained when the $\beta$-can structure is reformed. The onset of fluorescence can therefore be used as an indicator that the 11-strand $\beta$-barrel has been formed. GFP fluorescence is not observed until 90 min to 4 h after protein synthesis.[38,41] The protein folds quickly, but the subsequent fluorophore formation and oxidation is slow.[42] GFP refolding from an acid-, base-, or guanidine HCl-denatured state (chromophore containing but nonfluorescent) occurs with a half-life of between 24 s[43] and 5 min,[33] and the recovered fluorescence is indistinguishable from that of native GFP.[44]

*Aequorea* is found in the cold Pacific Northwest, and mature GFP, i.e., fully fluorescent GFP, is most efficiently formed at temperatures well below 37 °C. This has limited the uses of GFP and has led to the search for mutants that mature more efficiently at higher temperatures. Only soluble protein is fluorescent, and it has been suggested that incorrect folding often results in aggregation into insoluble inclusion bodies.[45] Since this misfolding has been blamed for the inefficient maturation, mutants designed for use at higher temperatures have been called folding mutants. They[41,46−51] reduce the ratio of proteins localized in inclusion bodies relative to wild-type GFP. The folding mutations can be divided into four groups: those that are buried and in close proximity to the chromophore, buried residues that are located far from the chromophore, surface mutations close to the chromophore, and surface mutations far from the chromophore.[52] Presumably folding mutations located close to the chromophore (e.g., S65A,G,T or L, and F64L and S72A) aid in chromophore formation, while those distant from it (e.g., V163A) are important in forming productive folding intermediates at higher temperatures.[52] Surface mutations (e.g., F99S/M153T/V163A) may aid in decreasing the surface hydrophobicity.[53] Unfortunately not all folding mutations act additively, thereby complicating the design of the most efficient folding mutant. Furthermore, it has been found that some GFP mutants with higher expression efficiencies have

increased mRNA transcription and translation efficiencies.[54] One of the most interesting recent findings has been that the folding rates of wild-type GFP and GFP mutants are different in bacteria and mammalian cells.[55] Since GFP most probably folds in the same way in all organisms, this difference in folding rate is presumably due to the influence of chaperones, which are known to bind GFP.[56,57]

The most widely studied of the folding mutants is the "Cycle3" mutant. It is a F99S/M153T/V163A mutant with a modified codon usage for better expression in *E. coli*, which was found by forming random mutations with PCR.[41] The folding and unfolding reactions of both wild-type and cycle3 mutants have been examined by fluorescence and circular dichroism spectroscopy, and the hydrogen-exchange reactions of both species have been compared by Fourier transform infrared spectroscopy.[53] Very few differences were observed between the cycle3 mutant and wild-type GFP. Both proteins have the same folding rates at 25 and 35 °C, and local structural fluctuations determined by hydrogen-exchange measurements are also the same in both proteins. The only difference found was that wild-type GFP has a greater tendency toward aggregation during refolding than the cycle3 mutant.[53] The difference in aggregation has been attributed to the replacement of two surface hydrophobic residues in GFP with two hydrophilic ones in the cycle3 mutant. The cycle3 mutant is more soluble than wild-type GFP in vivo at 37 °C. Thus, the authors concluded that decreased thermosensitivity of cycle3 is due to the reduced hydrophobicity on its surface and not improved folding.[53] The crystal structure of the cycle3 mutant has been solved. No significant differences between the cycle3 and wild-type structure were observed in the areas surrounding the mutations nor near the chromophore.[58] In vitro refolding experiments comparing the S65T and cycle3 revealed no differences between the two.[58]

On the other hand, the decreased thermosensitivity of GFPA in bacteria and yeast has been shown to be the result of its improved folding characteristics due to V163A and S175G mutations.[47] The oxidation of the chromophore of the same system was also shown to be temperature insensitive.[47] Compared with typical globular proteins, GFP was found to fold and unfold very slowly.[53]

Two single-point mutations, V163A and F64L, have been found that lead to higher yields of soluble fluorescent protein and improve the levels of fluorescence in mammalian cells grown at 37 °C.[59] Besides misfolding and aggregation, GFP chromophore formation at 37 °C might be inefficient because the carbonyl carbon of Ser65 is not held close enough to the amide nitrogen of Gly67 for a sufficient length of time and autocatalytic cyclization does not occur (see section V and Figure 5). Computational methods were used to find the low-energy conformations for the chromophore-forming regions of the immature V163A and F64L mutant. [In this paper we will refer to fluorescent chromophore-containing GFP as mature GFP and to the unmodified primary structure as immature GFP.] The distances between the carbonyl carbon of Ser65 and the amide nitrogen of Gly67 were found to be significantly shorter than those in the native GFP.[60]

The folding of $\beta$-sheets is not well understood. Because GFP only fluoresces once the chromophore is formed and that only occurs once the 11-strand $\beta$-barrel is formed, GFP is an excellent system to study $\beta$-sheet protein folding in vivo. An interesting application of this property has been the study of the effect of changing side-chain interactions between parallel $\beta$ strands of cycle3 GFP in vivo and in vitro.[61] A library of mutations at positions 17 and 122 was examined. These positions were mutated since they comprise a host−guest site between parallel $\beta$-strands in GFP. Absorption, fluorescence, and CD spectra of the mutants in vitro were very similar suggesting that the mutations did not change the structure of the chromophore. Although the mutants were expressed at comparable levels in *E. coli*, the rate and magnitude of fluorescence acquisition varied.[61] Therefore, the mutants have different ratios of protein in inclusion bodies and in the soluble fractions. Proteins that fold rapidly are protected from aggregation and are capable of forming the chromophore. Kinetics experiments in vitro showed large variation in refolding rates, while none were observed in the unfolding. Favorable cross-strand pairs were found to fold quicker and achieve higher final in vivo fluorescence than unfavorable host−guest interactions. Unfavorable interactions resulted in misfolding or partially folded protein aggregates. The in vivo and in vitro folding rates were found to be correlated.[62] The native cycle3 GFP host−guest pair was the most stable and folded the quickest.

Chaperones facilitate folding of proteins. One of the best understood chaperones is GroEL in *E. coli*. The link between fluorescence and the fully formed $\beta$-can has been used to show that denatured GFP refolds as quickly in the cavity formed by GroEL and GroES as it does by spontaneously refolding.[43] Fluorescence resonance energy transfer between a fused GFP and BFP in the cis-cavity of GroEL shows that the fusion protein fits in the cavity. A fusion protein made up of three GFPs does not fit.[56] The folding rates of wild-type GFP and GFP mutants are different in bacteria and mammalian cells;[55] this difference in folding rate is presumably due to the influence of chaperones.

A 1ns molecular dynamics simulation of wild-type GFP found that the protein was remarkably rigid, not only the $\beta$-barrel but also on an atomic scale around the chromophore.[63] This may be of importance to the protein's fluorescent behavior, see section VI.

The $\beta$-barrel and chromophore formation in GFP is strongly dependent on temperature, and deletion experiments[34,35] have shown that most of the protein is required for chromophore formation and fluorescence; however, rearrangements, insertions, and other major structural changes of GFP can still produce fluorescent GFP.[64−67] An extraneous loop made up of 20 amino acid residues has been inserted between residues 157 and 158 of GFP.[67] These residues are located in a loop on the surface of GFP. The resultant mutant was fluorescent, and one can therefore assume that folding was still able to occur.

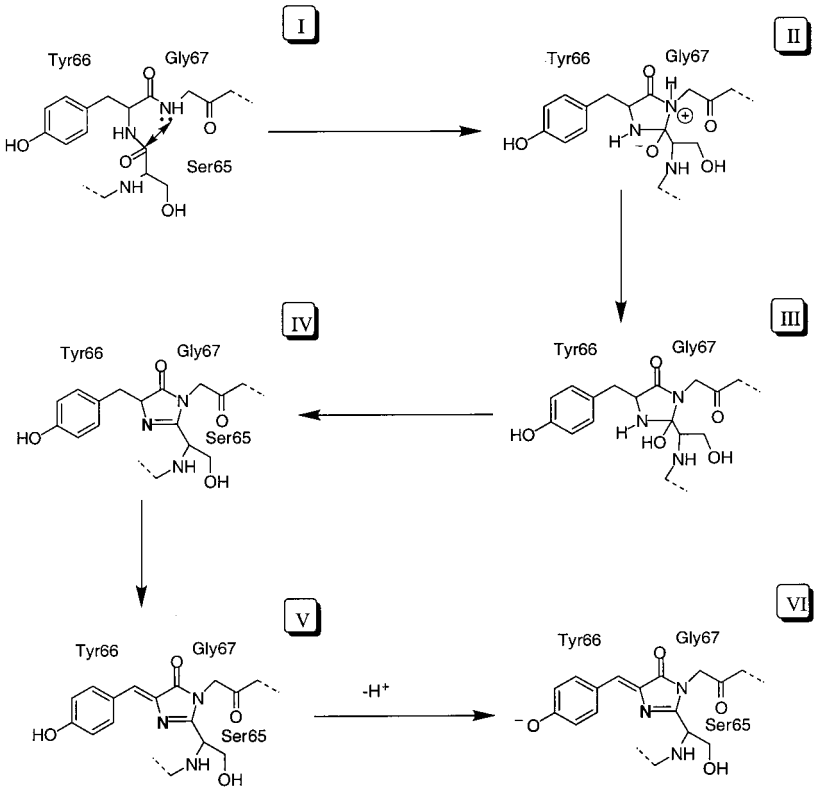


**Figure 5.** Proposed mechanism for the chromophore formation in Green Fluorescent Protein.[2,38]

The $\beta$-barrel found in wild-type GFP is resistant to proteolysis by both trypsin and Pronase despite the presence of putative cleavage sites in exposed folds of the structure. Insertion of the IEGRS pentapeptide at positions 157, 172, and 189 resulted in a GFP mutant that is cleaved by proteolytic enzymes.[68]

The sg100 GFP mutant (F64L, S65C, Q80R, Y151L, I167T, and K238N) was dissected at the same position, resulting in two separate strands of GFP. Fluorescence did not occur when the two GFP strands were expressed. However, when amino acid residues designed to form an antiparallel leucine zipper were added to both strands, fluorescence occurred upon expression in vivo and in vitro.[65] The antiparallel zipper joined the two strands in such a way that the heterodimer folded correctly and the chromophore was formed.[65]

The serendipitous finding that Y145 could be replaced with the FKTRHN hexapeptide fragment in EYFP (S65G, V68L, Q69K, S72A, and T203Y) without losing its fluorescence has led to the design of a number of circular permuted GFPs and GFPs in which proteins have been inserted in GFP, rather than being appended at the origin or end of GFP,[64] see Figure 10.

## V. Chromophore Formation

A most interesting feature of GFP is that its function is based on a chromophore formed through a rarely observed autocatalytic posttranslational cyclization of a peptide from its own backbone structure. Initially it was believed that the autocatalytic GFP cyclization was unique, but recent research has indicated that a family of enzymes, including histidine ammonia lyase (HAL) and the closely related phenylalanine ammonia lyase (PAL), also contain posttranslational ring formations that occur autocatalytically through the attack of the protein backbone on itself.[69,70]

The detailed mechanism for the formation of the chromophore in GFP is unknown. However, Tsien[2,38] proposed the autocatalytic biosynthetic mechanism shown in Figure 5.The scheme accounts for the spontaneous chromophore formation in a variety of GFP-expressing organisms which are unlikely to contain the same specific catalysts for the process. It also accounts for the fact that GFP maturation in an anaerobic environment results in a soluble protein (species IV in Figure 5) that has the same gel electrophoresis behavior as GFP but does not fluoresce. Addition of oxygen results in gradual fluorescence (species V and VI in Figure 5).[38] Chromophore formation in S65T was shown to occur in three distinct kinetic steps.[42] First, protein folding is fairly slow ($k_f = 2.44 \times 10^{-3}$ s$^{-1}$) and occurs before chromophore formation. Second, cyclization occurs ($k_c = 3.8 \times 10^{-3}$ s$^{-1}$), and finally the chromophore is oxidized in a slow step ($k_{ox} = 1.51 \times 10^{-4}$ s$^{-1}$),[42] see Figure 6. The rate of the oxidation step varies significantly in GFP mutants.[52] The S65T mutant is oxidized 5 times faster than wild-type GFP,[71] which in turn is significantly faster than the V163A/S175G mutant.[47]

On the basis of the computational analyses of the hexapeptide FSYGVQ, which were completed prior to the publication of the crystal structure of GFP, it was proposed[72,73] that the posttranslational chromophore formation occurs due to the presence of low-energy conformations which have very short intramolecular distances between the carbonyl carbon of

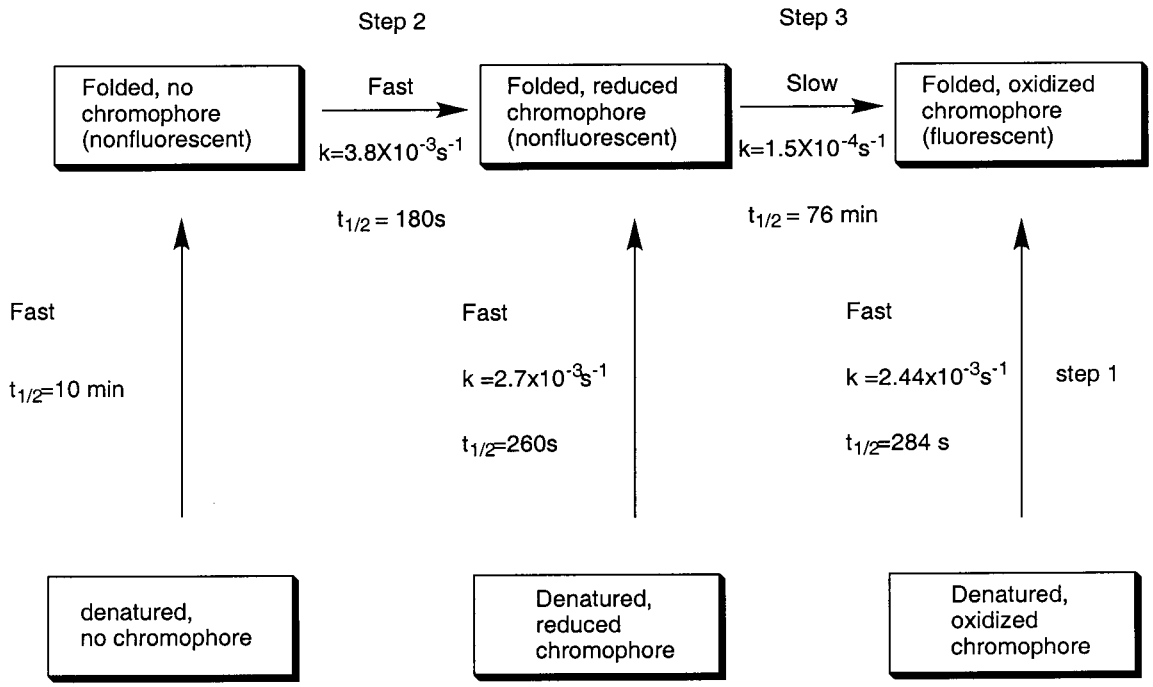


**Figure 6.** Kinetic pathway of chromophore formation in S65T. Protein folding is fairly slow ($k_f = 2.44 \times 10^{-3}s^{-1}$) and occurs before chromophore formation. It is followed by cyclization ($k_c = 3.8 \times 10^{-3}s^{-1}$) and chromophore oxidation.[42]

Ser65 and the amide nitrogen of Gly67 (↔ in I, Figure 5). It was also suggested that an arginine side chain may hydrogen bond to the carbonyl oxygen of Ser65, activating the carbonyl carbon of Ser65 for attack by the lone pair of the Gly67 amide nitrogen.[72,73] The close proximity of an arginine, namely, Arg96, was confirmed by the subsequent GFP crystal structures determinations. However, it may not be crucial to chromophore formation since mutants with no Arg96 reportedly do mature.[74]

Molecular mechanical conformational searches based on the wild-type crystal structure of GFP have shown that the chromophore-forming residues of immatureGFP are preorganized in a "tight turn" with the carbonyl carbon of Ser65 less than 2.90 Å from the amide nitrogen of Gly67.[60] Not only does the 11-stranded $\beta$-barrel enforce this "tight turn" that is required in chromophore formation, it also tremendously restricts the conformational space of the chromophore-forming region, so that the residues are kept in place for autocatalytic cyclization, a slow step ($t_{1/2} \sim 5$ min) in chromophore formation.[60]

Density functional calculations have led to the proposal that dehydration might precede cyclization in GFP.[75] The results obtained from these investigations indicate that the most commonly suggested mechanism (referred to as the reduced mechanism) is not energetically favorable but leads to large endothermicities for formation of the imidazolone ring and the required intermediate, irrespective of what chemical models and computational methods are used. This led to a proposal of an alternative mechanism where the cyclization is preceded by the dehydration of Tyr66 to dehydrotyrosine. This oxidized mechanism was found to be much more probable from an energetics point of view, resulting in a less unstable intermediate and reaction energies close to thermoneutral. The calculations also showed

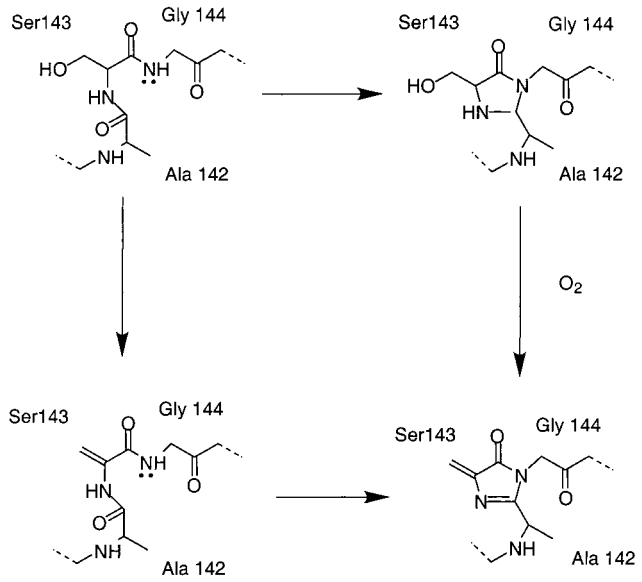


**Figure 7.** Proposed reaction sequence for the ring formation in histidine ammonia−lyase. The sequence going to the top right is the conventional reduced mechanism, while that going through the bottom left is the oxidized mechanism predicted by DFT calculations.[70]

that the analogy between the deamination step of Asn-Gly sequences in peptides and GFP chromophore formation is not energetically valid. Database searches showed that the oxidative mechanism in which the formation of the dehydro amino acids in residue i+1 precedes the cyclization is also structurally advantageous as it results in shorter distances between the carbonyl carbon of residue i and the amide nitrogen of residue i+2 and therefore preorganizes the protein for cyclization.[70] Many similarities were observed in the autocatalytic postranslation intramolecular cyclization in histidine ammonia-lyase (HAL) and GFP,[70] see Figure 7.

A lot more information about chromophore formation and GFP folding is hidden in the identity and location of the many mutants that result in a total loss of fluorescence. Unfortunately these "negative" results are rarely published.

## VI. Photochemistry

### A. Spectral Characteristics

Wild-type GFP has a major absorption at 398 nm[26] and a minor absorption at 475 nm with a shoulder on the red edge.[33,76] Excitation at 398 nm results in an emission maximum at 508 nm, while irradiation at 475 nm produces an emission with a maximum at 503 nm.[38] There seems to be little doubt that a change in protonation is responsible for the different absorptions; however, there is some controversy about the location of the acid- labile site. The 398 nm absorption is normally attributed to a neutral form of the chromophore ($HO_Y$,N,$O_X$, species A), the absorption at 475 nm to an anionic form ($^-O_Y$,N,$O_X$, species B),[77] and the red shoulder at 475 nm to a zwitterionic species ($^-O_Y$,$HN^+$,$O_X$, species I).[76] The anionic and neutral species are connected by a ground-state equilibrium, and their relative concentrations can be manipulated by changes in protein concentration, ionic strength, pH, temperature, and addition of cryoprotectors.[78−80] Excitation of either species A (neutral) or species B (anionic) results in a similar excitation spectra. This is presumably due to the fact that the phenolic oxygen of Tyr66 is more acidic in the excited state than in the ground state; excited-state proton transfer occurs resulting in a common anionic excited state that is responsible for the observed emission spectrum.[38,79,81] A computational analysis of the denatured GFP chromophore suggests that it can be found in five different protonation states over the pH range from −3.2 to 9.4.[82] At pHs over 9.4 it is in the anionic form, between 1.1 and 9.4 it is in an equilibrium between the neutral and the zwitterionic form, and it is in the cationic form ($HO_Y$,$HN^+$,$O_X$) for pHs between −3.2 and 1.1.[82] In the absence of oxygen, mature GFP rapidly turns red, absorbing at 525 nm and emitting at 600 nm.[83] The reason for this photophysical behavior is unknown.

Tsien[4] has written an excellent review in which he classified GFPs into seven major classes based on their spectral characteristics. They are as follows:

(i) Wild-type GFP. The chromophore is in an equilibrium between the phenol and phenolate form. It has two excitation peaks at 395 and 475 nm.

(ii) Phenolate anion (e.g., EGFP). Ser65 has been substituted with Thr, Ala, or Gly. Does not have the 395 nm excitation peak.

(iii) Neutral phenol (e.g., sapphire). Mutation of Thr203 to Ile results in a mutant that only has the 399 nm excitation. Presumably because the Thr alcoholic proton can no longer hydrogen bond to the phenolate, thereby stabilizing it.

(iv) Phenolate anion with stacked $\pi$-electron system (e.g., YFP). Mutation of Thr203 to His, Trp, Phe, or Tyr results in yellow fluorescent proteins.

(v) Indole in chromophore (e.g., CYP). Cyan fluorescent proteins have properties intermediate to those of BFP and EGFP.

(vi) Imidazole in chromophore and phenyl in chromophore (e.g., BFP). Blue fluorescent proteins have an excitation peak at 383 nm.

(vii) Phenyl in chromophore. This mutant has the shortest excitation wavelength and no apparent usefulness.[4]

The absorbance and fluorescence properties of the different classes are summarized in Table 3.

### B. Three-State Photoisomerization Model

On the basis of the observations discussed above and the fact that the Y66H mutant only absorbs at 384 nm,[38] changes in the absorption and fluorescence spectra that accompany other mutations, and the crystal structure of the Y66H mutant,[84] a mechanism, shown in Figure 8, for the photoisomerization of wild-type GFP was proposed.[36,38,59,81,84]

The neutral form of the chromophore can convert to the anionic species (B) by going through the intermediate state (I). In going from the neutral chromophore (species A) to the charged chromophore (B), the Tyr66 phenolic proton is shuttled through an extensive hydrogen-bonding network to the carboxylate oxygen of Glu222. The change from forms A to I is solely a protonation change, while the change from I to B is a conformational change with most changes occurring at Thr203. Spectral hole-burning experiments have shown that the ground state of form I is higher in energy than both the ground states of A and B and that it is separated from them by energy barriers of several hundred wavenumbers. In the excited state the barrier between A* and I* is low whereas that between I* and B* is at least 2000 $cm^{-1}$.[76] The mechanism shown in Figure 8 has been partially validated by the interpretation of the absorption and Stark spectra of the wild type, the S65T and Y66H/Y145F GFP mutants.[85] The electronic spectra show that the excitation of species A only involves a small charge displacement, while excitation of species B involves a significant change from the ground state. Since the intermediate state (I) is structurally similar to both the ground and excited state of species A and electronically similar to the ground and excited state of species B, the protein has to undergo structural changes in going from state A to state B. Additional evidence comes from the X-ray structure of S65T at low pH, which shows that there is no hydrogen-bonding interaction between the side chain of Thr203 and the phenolic oxygen of the chromophore, while the side chain $\chi_1$ dihedral rotates by 100° to form a hydrogen bond in the high pH structure.[86] Electrostatic calculations have been used to examine coupling of the ionization states of Thr203 and Glu222 and the related side chain reorientations.[87] The calculations correctly reproduced the coupling between the protonation state of the chromophore and the side-chain conformation of Thr203, which is shown in Figure 8. Molecular mechanics calculations and database analyses have been used to support the photoisomerization mechanism shown in Figure 8. They have also shown that the rotation

**Table 3. Spectral Characteristics[a] of Different Classes of Green Fluorescent Protein Mutants[52]**

| mutations | common name | quantum yield and molar extinction | excitation and emission max | relative fluorescence at 37 °C |
|---|---|---|---|---|
| | | i. S65T type | | |
| S65T, S72A, N149K, M153T, I167T | Emerald | $\Phi = 0.68$ | 487 | 100 |
| | | $\epsilon = 57{,}500$ | 509 | |
| F64L. S65T, V153A | | $\Phi = 0.58$ | 488 | 54 |
| | | $\epsilon = 42{,}000$ | 511 | |
| F64L, S65T (EGFP) | EGFP | $\Phi = 0.60$ | 488 | 20 |
| | | $\epsilon = 55{,}900$ | 507 | |
| S65T | | $\Phi = 0.64$ | 489 | 12 |
| | | $\epsilon = 52{,}000$ | 511 | |
| | | ii. Y66H type | | |
| F64L, Y66H, Y145F, V163A | P4−3E | $\Phi = 0.27$ | 384 | 100 |
| | | $\epsilon = 22{,}000$ | 448 | |
| F64L, Y66H, Y145F | | $\Phi = 0.26$ | 383 | 82 |
| | | $\epsilon = 26{,}300$ | 447 | |
| Y66H, Y145F | P4−3 | $\Phi = 0.3$ | 382 | 51 |
| | | $\epsilon = 22{,}300$ | 446 | |
| Y66H | BFP | $\Phi = 0.24$ | 384 | 15 |
| | | $\epsilon = 21{,}000$ | 448 | |
| | | iii. Y66W type | | |
| S65A, Y66W, S72A, N146I, M153T, V163A | W1C | $\Phi = 0.39$ | 435 | 100 |
| | | $\epsilon = 21{,}200$ | 495 | |
| F64L, S65T, Y66W, N146I, M153T, V163A | W1B | $\Phi = 0.4$ | 434 452 | 80 |
| | | $\epsilon = 32{,}500$ | 476 (505) | |
| Y66W, N146I, M153T, V163A | W7 | $\Phi = 0.42$ | 434 452 | 61 |
| | | $\epsilon = 23{,}900$ | 476 (505) | |
| Y66W | | | 436 | n.d. |
| | | | 485 | |
| | | iv. T203Y type | | |
| S65G, S72A, K79R, T203Y | Topaz | $\Phi = 0.60$ | 514 | 100 |
| | | $\epsilon = 94{,}500$ | 527 | |
| S65G, V68L, S72A, T203Y | 10C | $\Phi = 0.61$ | 514 | 58 |
| | | $\epsilon = 83{,}400$ | 527 | |
| S65G, V68L, O69K, S72A, T203Y | 10C Q69K | $\Phi = 0.71$ | 516 | 50 |
| | | $\epsilon = 62{,}000$ | 529 | |
| S65G, S72A, T203H | | $\Phi = 0.78$ | 508 | 12 |
| | | $\epsilon = 48{,}500$ | 518 | |
| S65G, S72A, T203F | | $\Phi = 0.70$ | 512 | 6 |
| | | $\epsilon = 65{,}500$ | 522 | |
| | | v. T203I type | | |
| T203I, S72A, Y145F | H9−40 | $\Phi = 0.64$ | 399 | 100 |
| | | $\epsilon = 29{,}000$ | 511 | |
| T203I | H9 | $\Phi = 0.6$ | 399 | 13 |
| | | $\epsilon = 20{,}000$ | 511 | |
| | | vi. wild type | | |
| none or Q80R | wild type | $\Phi = 0.79$ | 395 | 6 |
| | | $\epsilon = 25{,}000$ | 504 | |
| | | $\epsilon = 9500$ | 470 | |
| F99S, M153T, V163A | cycle 3 | $\Phi = 0.79$ | 397 | 100 |
| | | $\epsilon = 30{,}000$ | 506 | |
| | | $\epsilon = 6500$ | 475 | |
| | | vii. phenyl in chromophore | | |
| Y66F | | | 360 | |
| | | | 442 | |

[a] Reprinted with permission from ref 52. Copyright 1999 Academic Press.

of the Thr203 side chain is restricted due to its location in a LSTQS sequence.[88]

Low-temperature optical investigations down to 2K were able to find conformations of GFP that are only transiently populated at room temperature. Three new photoproducts were found, one corresponding to A* (489 nm) and two to I* (502 and 510 nm).[89]

In GFP mutants with no detectable absorption of the neutral chromophore, such as the E222Q mutant, the neutral state still seems to play an important role in the photodynamics of GFP.[90]

## C. Twisted Excited-State Chromophore

At neutral or acidic pH, denatured wild-type GFP absorbs at 384 nm ,while in alkali pH it absorbs at 448 nm, but neither denatured GFP,[91] the chromophore-containing hexapeptide fragment,[29,92] nor synthetic model compounds[77,93,94] fluoresce. The denatured GFP and the hexapeptide fragment do however become highly fluorescent at 77 K, indicating that inhibition of vibration or rotation around the exo-methylene double bond of the chromophore pre-

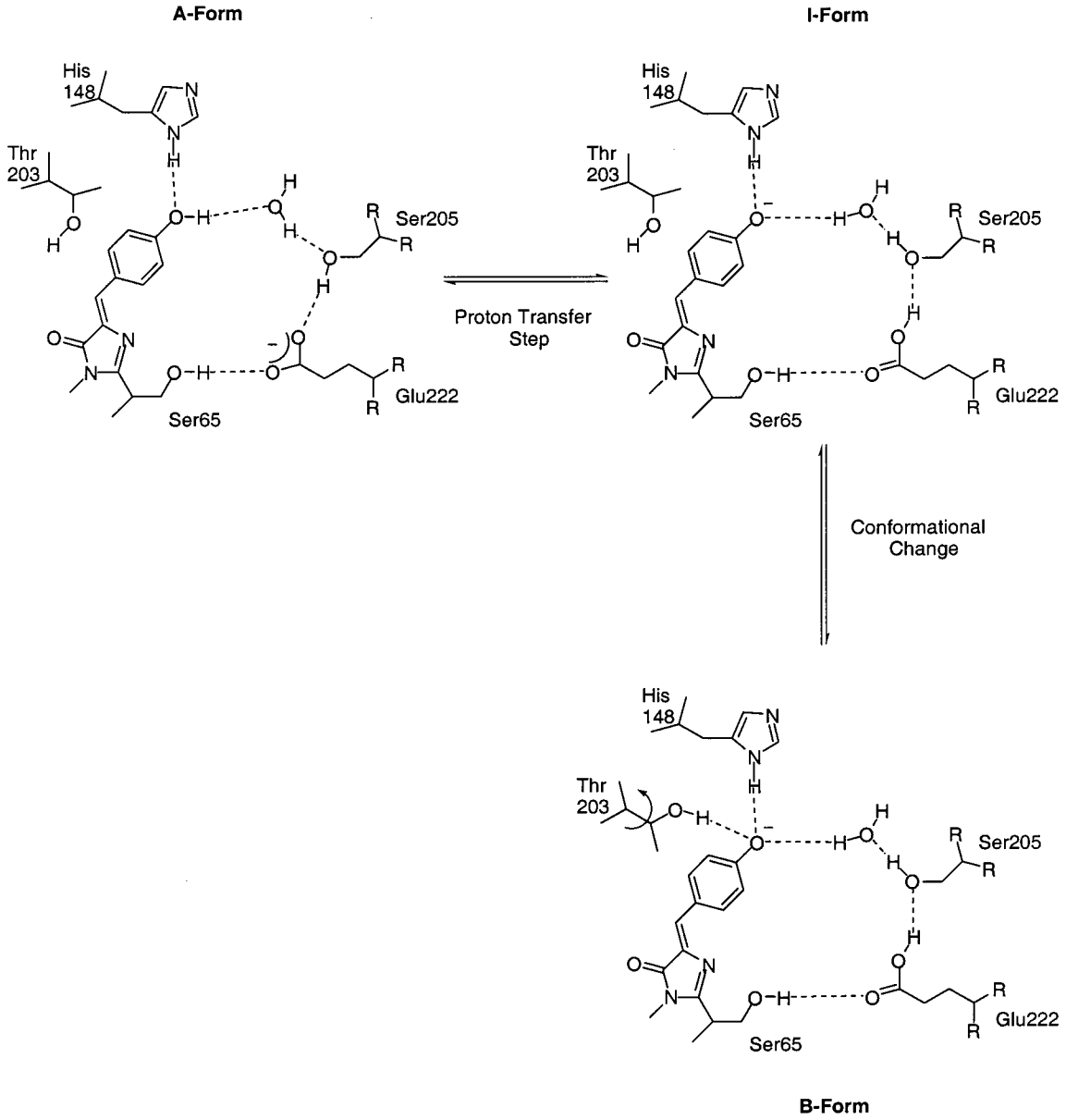


**Figure 8.** Proposed mechanism for the photoisomerization of wild-type GFP. The neutral form of the chromophore (A) can convert to the anionic species (B) by going through the intermediate state (I). In going from the neutral species (A) to the charged species (B), the Tyr66 phenolic proton is shuttled through an extensive hydrogen-bonding network to the carboxylate oxygen of Glu222. The change from forms A to I is solely a protonation change, while the change from I to B is a conformational change with most changes occurring at Thr203.

vents reduction in fluorescence due to fast internal conversion.[7,95] Wild-type GFP has a fluorescence quantum yield ($\Phi_f$) of 0.8,[26] while the isolate chromophore in solution has a quantum yield of $10^{-3}$.[77]

Quantum mechanical calculations[96] have been carried out for the ground and excited states of a number differently protonated forms of a GFP gas-phase model chromophore with $\tau$ and $\varphi$ dihedral angles having values of 0°, 90°, and 180°, see Figure 2. Electronic excitation ($S_0 \rightarrow S_1$) was found to alter the conformation of the chromophore. For the cationic model (species A = $HO_Y$,$HN^+$,$O_X$) a $\tau$ dihedral angle of 90° was an energy maximum in the ground state and an energy minimum in the excited state. On the basis of these findings the authors proposed that the loss of fluorescence in some of the red-shifted mutants is due to fast internal conversion from the perpendicular excited-state structure of the protonated chromophore and that this perpendicular orientation is sterically prohibited in most GFPs, see also sections VI.D and VI.G.

Molecular mechanics and dynamics simulations have shown that GFP has a fairly large central cavity, which contains the chromophore; however, it does not have a shape that is complementary with a planar chromophore.[97] The protein exerts some strain on the chromophore when it is planar, and the only reason planar chromophores are found in GFP is due to their delocalized $\pi$-electrons. The protein environment of GFP allows the chromophore some rotational freedom, especially by a hula-twist and in the $\varphi$ dihedral angle.[97] The excited state, responsible for fluorescence, may therefore be twisted relative to the ground state. However, cis−trans photoisomerization cannot occur by a 180° rotation of the $\tau$ dihedral angle.[97]

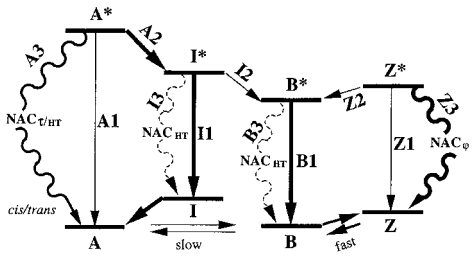


**Figure 9.** Model for the photophysical behavior of GFP. Excited states are labeled by asterisks. Barriers may exist for processes of types 2 and 3. Excitation arrows have been omitted for simplicity. The relative free energies of the ground-state forms A (neutral), B (anionic), I (intermediate), and Z (zwitterionic) depend on the protein environment. (Reprinted with permission from ref 99. Copyright 1999 National Academy of Sciences, U.S.A.).

The results from recent fluorescence and ultrafast ground-state recovery studies of synthetic GFP analogues are not consistent with the theory that fast internal conversion occurs through large-scale torsional rotation in the excited state.[98]

## D. Four-State Photoisomerization Model

Quantum mechanical calculations have also been used to develop a model that explains the short- and long-lived "dark" states (described in section VI.F) and the relaxed excited-state decay channels in GFP.[99] The model, see Figure 9, is an extension of the three-state model[81,95] for the photophysical behavior of GFP shown in Figure 8.

A cis−trans photoisomerization and a zwitterionic form, Z, have been added to the three-state model. In some of these forms the ground- and excited-state adiabatic potential surfaces come very close to each other, which can facilitate nonadiabatic crossing (NAC). Radiationless decay through NAC is the preferred decay channel for the zwitterionic form. The isomerization can occur around the $\tau$ and $\varphi$ dihedral angles as well as by a concerted hula-twist of both the $\tau$ and $\varphi$ dihedral angles.[99] Therefore, it has been suggested that the Z form is "dark" in fluorescence. The excited states of the neutral (A*), intermediate (I*), and anionic (B*) species undergo minimal radiationless decay through NAC. Parts of the mechanism shown in Figure 9 have been confirmed by time-resolved spectroscopy studies that have determined the fluorescence lifetimes of the I and B species and have shown that the irreversible photochromomicity observed between species A* and B* is due to the formation of the excited state of species B which cannot return to any other species in the ground state.[100] The A and I ground states were found to be in thermal equilibrium.

## E. Evidence That Does Not Support the Three- or Four-State Model

Two studies have reported results that do not support the photoisomerization mechanism and charge distribution shown in Figures 8 and 9. An infrared study of both forms of $GFP_{UV}$ found that photoisomerization involved a change in protonation, but that the protonation state of Glu222 remains unchanged, and that the Thr203 side chain was in the same conformation in both the A and B forms.[101] However, an ab initio theoretical study of the ground electronic state structures and their vibrational spectra in selected protonation states suggests that the neutral from of Glu222 may be present in the above-mentioned FTIR difference spectrum[102] but might be partially obscured. A systematic study of aliphatic Thr203 mutants has shown that the excited-state proton transfer shown in Figure 8 can occur without Thr203.[103]

Good agreement between the predicted and observed absorption spectra were obtained in quantum mechanical calculations when species A was modeled by a cationic ($HO_Y$,$HN^+$,$O_X$) form and species B by the zwitterionic ($O_Y^-$,$HN^+$,$O_X$), see Figure 2.[104,105]

When examining the mechanism shown in Figure 9 and discussed above it is important to remember that no experimental evidence for the zwitterionic and cationic species are known.[106] In fact, a Raman study of a model chromphore and of the chromophore in wild-type and S65T GFP revealed that the cationic species ($HO_Y$,$HN^+$,$O_X$) is not found for wild-type and S65T GFP.[106] Nor was any evidence found for the presence of the zwitterionic species ($O_Y^-$,$HN^+$,$O_X$). The ground-state structure of the neutral form of the chromophore (species A) was found to be insensitive to the chromophore environment, while anionic form (species B) is strongly dependent on the chromophore environment.[106] Resonance Raman spectroscopy is useful because the vibrational modes that are enhanced most strongly are those for which the excited state is shifted significantly relative to the ground state. In GFP the C═N and C═O bonds are most strongly coupled to optical excitation with little contribution from the phenolic OH.[107] The same study also showed that the resonance Raman spectra of a model chromphore and the chromophore in GFP were substantially different, suggesting that the protein environment modifies the excited-state potential energy surface.[107]

## F. Photochemical Behavior of Single Green Fluorescent Protein Molecules

When GFP molecules are observed individually they display on/off blinking and switching behavior.[108−112] The on/off blinking occurs on time scales on the order of 1 s. After emitting a certain number of photons, GFP switches off to a dark state with a lifetime of about 5 min.[108] The dark state is different than the off-blinking behavior. The blinking has been shown to be photoinduced,[110] and it has been proposed that a reversible transition between the emitting anionic form and a dark intermediate state of an unknown identity is responsible for this behavior.[108] Two dark states have been observed for the E222Q mutant. One of the dark states has been identified as the neutral form of the chromophore (species A in Figure 8), and the other is presumably a triplet state.[90,113] Although the fluorescence spectra of bulk EGFP (F64L/S65T) are strongly dependent on pH, the duration of single EGFP-fluorescence bursts are independent of pH, suggesting that blinking is probably not due to switching between two protonation states of the chromophore.[109]

Although single-molecule studies in vivo are still a challenging task, EYFP appears to be the best GFP mutant for dynamically tracking single molecules. This is due to its resistance to photobleaching, detection ratio, and brightness.[114]

An enhanced YFP mutant, termed $E^2$GFP, has been obtained that might be used as a single-biomolecule optical switch.[115] As with most GFP molecules, prolonged or intense excitation results in photobleaching (at 476 nm in $E^2$GFP). However, $E^2$GFP is the only know mutant in which irradiation of the dark photobleached state (at 350 nm) forms an excited state that photoconverts to the anionic B form, which is fluorescent.

### G. Photodynamics of Yellow Fluorescent Protein (YFP) and Related Thr203 Mutants

The first mutants that were designed on the basis of the S65T crystal structure are yellow emission mutants (YFP) that have replaced Thr203 with aromatic amino acids.[31,108,116] The crystal structure of YFP (T203Y/S65T/V68L/S72A) has been solved;[116] it shows that Tyr203 and the chromophore are coplanar and that $\pi$-stacking occurs between the chromophore (Tyr66) and Tyr203. The structure has a hydrogen bond between Glu222 and the chromophore nitrogen, suggesting a neutral imidazolidinone ring nitrogen and a protonated Glu222 side chain.[116] The YFPs have the most red-shifted absorption of all currently known GFP mutants.[31,103] The red shift might be due to $\pi$-stacking; however, that would not explain why the absorption of the anionic form (species B) is shifted as far 529 nm while the absorption of the neutral form (species A) is nearly unchanged. YFPs have lower fluorescent quantum yields than GFPs, especially when the 475 nm band is excited.[95] This might be due to an increase in the conformational freedom of the $\tau$ and $\varphi$ dihedral angles of the chromophore resulting in faster decay.[99] Citirine, a third-generation YFP mutant (S65G,-V68L,Q69M,S72A,T203Y), is less sensitive to pH and chloride than YFP and has better photostability and expression at 37 °C than YFP.[117]

Fast excitation-driven dynamics in the fluorescence emission of YFP were examined by fluorescence correlation spectroscopy.[118] Excitation of the yellow-shifted mutants T203Y, T203F, and perhaps EGFP at high pH results in a bright excited state that is in equilibrium with two photophysically distinct dark (nonfluorescent) states. The one dark state is the protonated chromophore, but the other dark state does not involve protonation of the phenolate,[118] but it could be the dark zwitterionic species in four-state photoisomerization model shown in Figure 9. These dark states reduce the quantum efficiency and thereby negatively affect the utility of GFP.

Mutating Thr203 to aliphatic residues disrupts the hydrogen-bonding network shown in Figure 8 without introducing $\pi$-stacking. Some Thr203I mutants have almost no B band because the Tyr66 anion is no longer stabilized by Thr203,[38,119] while others still have a B band although it has been red shifted to 507 nm.[120] A systematic study of aliphatic Thr203 mutants has shown that the excited-state proton transfer shown in Figure 8 can occur without Thr203.[103] Furthermore, the $\pi$-stacking observed in YFP and discussed above is not responsible for the red shift as it also occurs in aliphatic mutants such as T203V.[103] Since the red shift is not due to $\pi$-stacking, an alternative hypothesis has been presented, namely, that changes in the charge distribution of the chromophore are responsible for the red shift.[103,121]

## VII. Applications

GFP fluorescence has been used to investigate a remarkable array of properties and behaviors. The main reasons for this are that the chromophore of GFP is produced through an internal posttranslational autocatalytic cyclization that does not require any cofactors or substrates, fusion of GFP to a protein rarely affects the proteins activity or mobility, and GFP is nontoxic in most cases. High GFP concentrations have been reported to have some toxicity in retroviral packaging cells[122] and in a few other cases.[123] However, there is some doubt about these findings.[124] GFP is resistant to heat, alkaline pH, detergents, photobleaching, chaotropic salts, organic salts, and many proteases.[125] Mutants with optimized codon usage for mammals,[2,51] plants,[126,127] yeast,[128] and fungi[129] have been created. Recently it has also been shown to retain fluorescence up to pressures of 600 MPa without any loss of fluorescence intensity.[125] GFP's large two-photon absorption make it an attractive candidate in applications such as data storage, diagnostics, and other photochemical applications.[130]

Some of GFP's limitations are the slow posttranslational chromophore formation, the oxygen requirement, and difficulty in distinguishing GFP from background fluorescence when the GFP is not densely localized or highly expressed.

Reviews of GFP applications studying protein dynamics in living cells,[131] using fluorescence microscopy,[132] GFP as a reporter gene,[8] techniques for distinguishing GFP fluorescence from endogeneous autofluorescence,[133] GFP applications in cell biology and biotechnology,[9] applications in plants,[6,134] in transgenic plants,[135] in fungal biology,[129] in bacterial protein localization,[136] in mouse embryos,[137] visualizing protein dynamics in yeast,[138] real-time molecular and cellular analysis,[10] GFP as a vital marker in mammals,[139] and GFP fusion constructs in gene therapy research[124] have been published. GFP fusions to detect apoptosis have been constructed and reviewed.[140] *Trends in Cell Biology* has recently started a series of review articles on the uses of GFP in a variety of applications and technologies. The first three reviews in the series have been entitled "Imaging biochemistry inside cells",[141] "Visualizing chromosome dynamics with GFP",[142] and "Lighting up the cell surface with evanescent wave microscopy".[143]

The GFP application most commonly known to the nonscientist in the United States is probably the production of ANDi, a transgenic rhesus monkey carrying the GFP gene.[144] ANDi made the nightly news shows, *New York Times*, and the Leno and Letterman shows. In France the production of a transgenic albino "GFP bunny" as part of a trans-

genic artwork[145] created a public outcry that resulted in the rabbit not being allowed to leave the country. The production of transgenic animals such as mice,[146] rabbits, and monkeys[144] has attracted public attention and resulted in the formation of small companies proposing to produce fluorescent pets, christmas trees, and flowers.[147] Green mice and other animals have been used as a source of green-tagged cells or organs for transplantation to make chimeric mice.[139] GFP has found many uses outside the laboratory, for example, it has been used in monitoring meat fermenting lactobacilli in sausages[148] and in tracking the spread of bacteria that consume diesel fuel in soils.[149] In the followings sections a summary of GFP laboratory applications is presented.

## A. Fusion Tags

A fusion between a cloned gene and GFP can be created using standard subcloning techniques. The resultant chimera can then be expressed in a cell or organism. In this way GFP fusion tags can be used to visualize dynamic cellular events and to monitor protein localization.[131,132] GFP is ideally suited as a fluorescent fusion protein marker because it does not require the presence of any cofactors or substrates. The chromophore is produced in vivo, and in most cases the resultant chimera does not affect the localization or activity of the tagged protein. For this reason GFP fusion proteins have been the most common and successful application of GFP in biotechnology.[9,131,150−153] GFP migration from cell-to-cell has been observed; in some cases this was due to nonspecific GFP diffusion.[154] GFP fusion markers have been used in many organisms ranging from viruses[155] and *Xenopus*[156] to mammalian cells.[157] The list of successful GFP fusions reported in the literature is very large. In 1995 Tsien published a table of successful fusions[2] which was supplemented by a listing of most major organelles targeted by GFP.[150]

Most GFP chimeras have been created by fusing the protein of interest to the amino or carboxyl termini of GFP. This does not have to be the case; GFP with its coding sequence intact has successfully been inserted into a host protein.[158,159] Because the amino and carboxyl termini of GFP are located close to each, they can be connected by a peptide linker and circular permuted. GFP can be created with new carboxy and amino termini in 10 different positions. The original EGFP can be interrupted at E142, Y143, Y145, H148, D155, H169, E172, D173, A227, and I229.[64] Circular-permuted GFP (cpGFP) that was interrupted at Y145 has successfully been fused to proteins at its termini.[64] The cpGFPs have altered p$K_a$s as well as different conformations of the chromophore relative to the fusion protein. Figure 10 shows the possible topologies of GFP, cpGFP, and chimeras with other proteins.

To establish why most proteins fused to GFP still retain their function, the motional dynamics of a GFP fusion construct were examined by fluorescence correlation spectroscopy and time-resolved fluorescence anisotropy.[160] The rotational correlation time of the construct, a single-chain antibody fused to GFP, was too short to be due to a globular rotation of the whole molecule. Instead, the GFP and fusion protein were found to behave independently, in a manner similar to that observed prior to fusion.[160] A fast hinge motion probably occurs between the two fused proteins, and there is no steric interference between the two partners. The length of the polypeptide linker can affect the stability of GFP fusion proteins.[161]

## B. Reporter Gene

The first applications of GFP were as a reporter gene.[20] Gene expression can be monitored by using a GFP gene that is under the control of a promoter of interest and measuring the GFP fluorescence which directly indicates the gene expression level in living cells or tissue. Green fluorescent protein has been extensively used as a reporter gene,[162−166] especially in spatial imaging of gene expression in living cells.[8,167−173] However, its low sensitivity, due to the fact that there is no signal amplification, because each GFP has only one chromophore, has limited its use somewhat. The low sensitivity can be overcome by using sensitive photon counting devices;, however, they are too expensive for routine uses.[9] The slow posttranslational chromophore formation also limits the use of GFP in the study of fast transcriptional activation processes. Another difficulty in using GFP is the nonlinearity of the fluorescent signal, which necessitates the determination of new calibration curves in each new application. A destablized form of GFP has been generated for applications in studies that require rapid reporter turnover.[174]

## C. Fluorescence Resonance Energy Transfer (FRET)

Fluorescence resonance energy transfer (FRET) is a nonradiative exchange of energy from an excited donor fluorophore to an acceptor fluorophore that is within 10−100 Å from the donor. In order for FRET to occur, the emission spectrum of the donor has to overlap with the excitation spectrum of the acceptor. The emission and excitation spectra of BFP and GFP overlap as do the spectra of CFP and YFP, making them good potential FRET pairs. The efficiency at which the Foerster-type energy transfer occurs is steeply dependent ($1/r^6$) on the distance between the fluorophores. Because any biochemical signal that changes the distance or orientation between the two fluorophores will affect the efficiency of FRET, it is a very useful technique for studying protein−protein interactions in vivo and in vitro.[5,132,150,175−177] The use of GFP in FRET-based applications has recently been reviewed.[132,141,178] Some of the reasons spectral variants of GFP have not been used as FRET partners more frequently are that they fluoresce with relatively low intensity, the emission spectra of the donor and acceptor pairs are not fully separated, and the chromophore is deeply buried within GFP (∼15 Å). One of the first uses of FRET was as a calcium probe.[179,180] This use is described more fully in section VII.E, which describes some of the ways FRET and other GFP-based techniques have been used to determine calcium concentrations. FRET has also been used to study protein−protein interactions.[181−184]

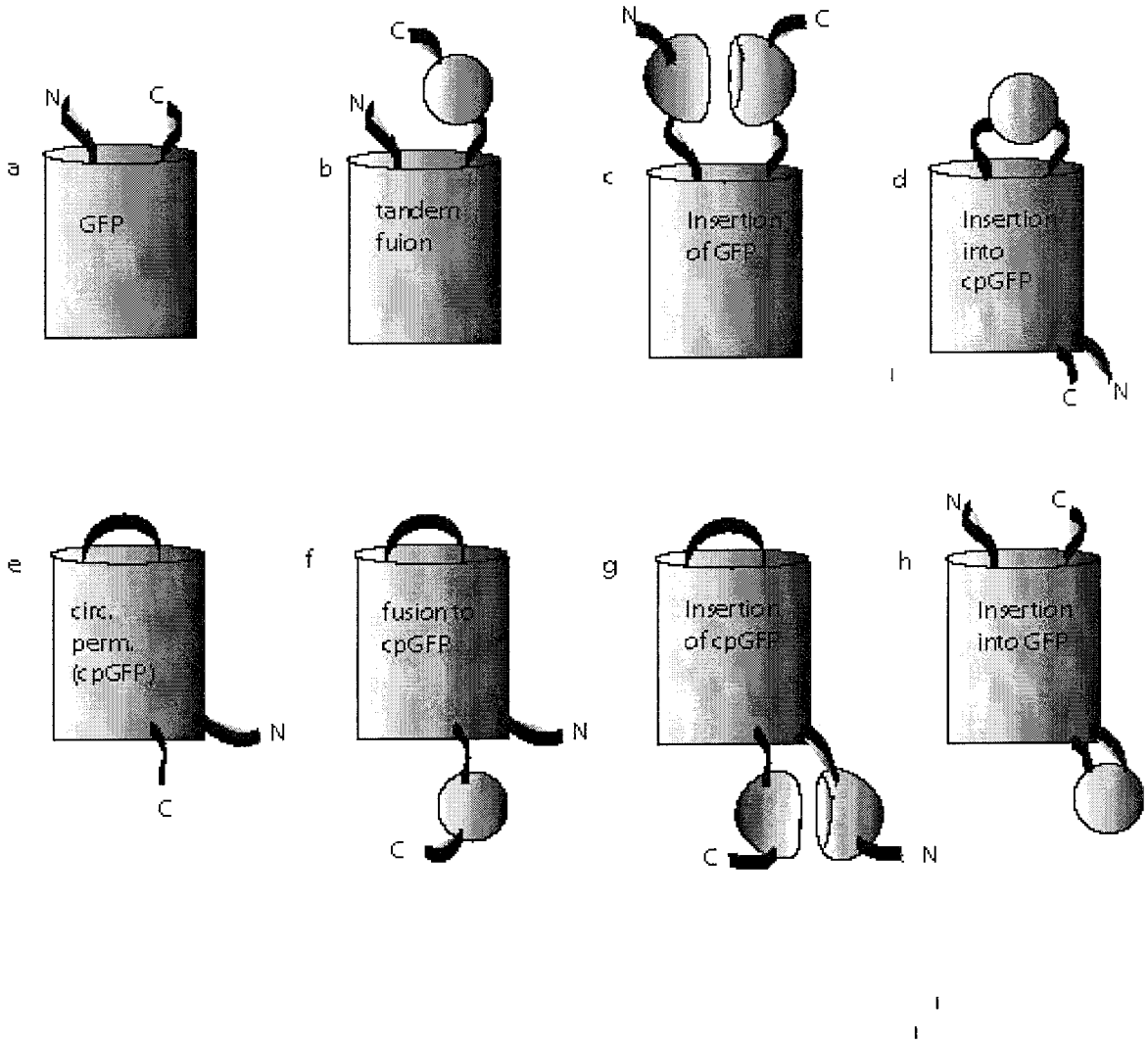


**Figure 10.** Possible topologies of GFP, cpGFP, and their chimeras with other proteins. Proteins are depicted as spheres or hemispheres when GFP or cpGFP is inserted within the protein.[64]

Recently a FRET imaging technique that circumvents the need for the use of two spectrally distinct FRET partners has been published.[185] Fluorescent lifetime imaging microscopy (FLIP) was successfully used to determine the fluorescence lifetime of the FRET donor/acceptor emission of a EYFP/EGFP pair that were spectrally similar and previously unusable for FRET.[185] GFP has also been used in FRET-based applications with other non-GFP partners.[186] Low-temperature high-resolution spectroscopy[187] of S65T, RS-GFP, and EYFP have shown that they are not photostable one-color systems as previously thought. Just like wild-type GFP, they can be photoconverted between at least three conformations.[187] This might be of significance in FRET studies as the emission observed in FRET experiments may be due to a photoinduced conversion between conformers of the excited state and not due to resonance energy transfer.[187]

The use of FRET to follow the conformational changes involved with metal release from metallathionein[188] is typical of FRET applications based on the concept that a conformation change of a peptide sequence between a FRET pair will change the distance between them and their relative orientations and thereby change the FRET. It will be used to illustrate the technique. The concept has been applied in calcium ion indicators[179,180,189] and protease[50,183,190] and kinase[191] activity monitoring. Upon reacting with NO (or a secondary product), metallathionein releases zinc or cadmium. A cyan GFP mutant (donor) and a yellow GFP (acceptor) were fused to the amino and carboxy termini of metallathionein. The resultant fusion protein (FRET-MT) retained its ability to bind metal ions. Upon addition of ethylenediaminetetraacetic acid (EDTA) and NaCl, FRET-MT released zinc and the protein unfolded, resulting in a drop in the $F_{535nm}/F_{480nm}$ emission ratio. Similar behavior was observed on addition of an aqueous solution of NO to a cell lysate containing FRET-MT. Therefore, the change in conformation upon metal release can be monitored by FRET, which reveals changes in the intramolecular distance and relative orientation of the fluorophores in CFP and YFP,[188] see Figure 11.

## D. Photobleaching

Photobleaching can be used to investigate protein dynamics in living cells. There are two methods based on photobleaching: fluorescence recovery after pho-

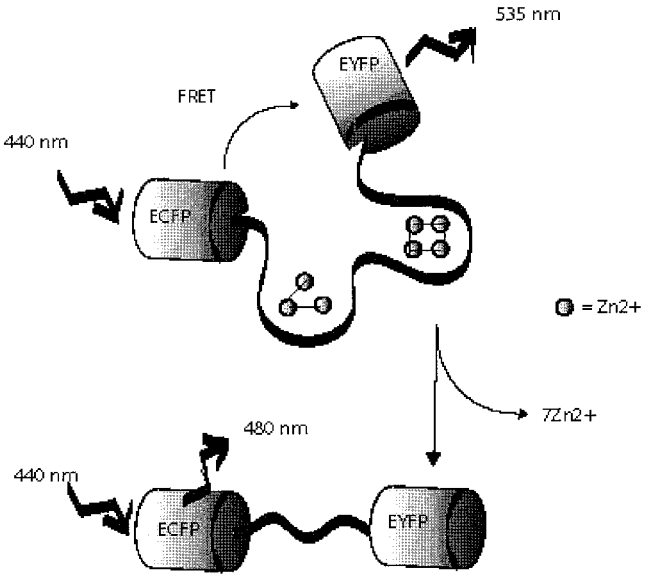


**Figure 11.** Example of a typical use of FRET to monitor conformational changes. When the FRET-MT construct is bound to metal ions, it is tightly folded and FRET between ECFP and EYFP occurs. Upon metal release the FRET-MT construct unfolds and a reduction in FRET occurs.[188]

tobleaching (FRAP) and fluorescence loss in photobleaching (FLIP). By illuminating an area with high-intensity illumination (bleaching) and monitoring the recovery of the resultant fluorescence loss (FRAP), the relative mobility of the GFP chimera can be determined. FLIP can be used to study transport of GFP fusion proteins between different organelles by repeatedly bleaching an area and monitoring the loss of fluorescence from outside the area. Applications of photobleaching GFP in cell biology have been reviewed.[192,193]

Photobleaching in YFP has been shown to be a ground-state thermal process, not an excited-state reaction.[194]

## E. Calcium

Numerous applications of GFP-based calcium indicators have been reported.[195−199] The GFP-based calcium reporter techniques can be divided into four groups.

### *1. Cameleons*

Cameleon constructs are composed of two GFP mutants (CFP and GFP or YFP) linked by calmodulin, which in turn is fused to a calmodulin-binding peptide (M13).[179,180] In the absence of calcium, the two GFPs are well separated. However, upon binding calcium, the calmodulin wraps around its target peptide (M13) and brings the two GFP mutants closer together, thereby increasing FRET. These constructs have been called cameleons because they change color and have a long tongue (M13) that retracts and extends in and out of the calmodulin mouth.[200] A similar construct has been made by fusing two GFP mutants (BFP and GFP) to a short calmodulin binding peptide.[189] Binding of calcium−calmodulin separates the two GFP mutants, resulting in decreasing FRET. The system responds to calmodulin-bound calcium and not to $Ca^{2+}$ itself.

Despite the fact that DsRed is an obligate tetramer and that it has a broad absorption spectrum with several shoulders, a red cameleon tolerant of acidosis has been created using a sapphire−DsRed FRET pair.[201]

### *2. GFP-Aequorin Bioluminescent $Ca^{2+}$ Reporters*

In single-cell applications the FRET-based cameleons have to be present in sufficiently high concentrations to be distinguishable from background autofluorescence[133] and calcium-independent electron transfer. By fusing GFP and aequorin. a calcium reporter molecule has been created[202] that is able to show increases in cytosolic $Ca^{2+}$ at a single-cell level. The chimera combines the calcium sensitivity of aequorin and the fluorescence of GFP.

### *3. Camgaroo*

Calmodulin has been inserted at position 145 of cpECFP, cpEGFP, and cpEYFP; all resulted in $Ca^{2+}$-sensitive proteins, called camgaroos.[64] The EYFP construct is the most sensitive to $Ca^{2+}$ and has been used to monitor cytosolic $Ca^{2+}$ concentrations in single mammalian cells. A disadvantage of camgaroos is that they rely on changes in the emission caused by altered p$K_a$s and are therefore pH sensitive. They have been called camgaroos because they are yellowish, carry a smaller companion (calmodulin) inserted in their pouches, can bounce high in signal, and may spawn improved progeny.[64] Recently a new generation of camagaroos has been developed using citirine.[117]

### *4. Pericams*

Pericams are chimeras constructed from circularly permuted green fluorescent protein (cpEYFP, see section VII.A). A calmodulin-binding peptide (M13) is bound to the new N terminus, and calmodulin itself is bound to the new C terminus.[66,203] Three types of pericams have been reported: flash-pericams become brighter with $Ca^{2+}$, inverse pericams become dimmer in the presence of $Ca^{2+}$, and ratiometric-pericams have an excitation wavelength that changes in a $Ca^{2+}$-dependent manner. The pericams differ in amino acid mutations close to the chromophore.

## F. Halides

YFP has been shown to be sensitive to both pH and various anions.[204] The p$K_a$ of YFP−H148G in the absence of $Cl^-$ has been shown to be 7.14; it increased to 7.86 at 150mM $Cl^-$.[205] The anion selectivity sequence for fluorescence quenching of YFP−H148Q was found to be $ClO_4^- \sim I^- > SCN^- > NO_3^- > Cl^- > Br^-$ > formate > acetate. The fluorescence quenching is due to protonation of the chromophore upon anion binding.[206] The crystal structures of both the apo- and $I^-$-bound YFP−H148Q mutants have been solved.[206] The iodide ion was found in a small cavity adjacent to Arg96, which provides electrostatic stabilization. It was also within van der Waals contact of the chromophore imidazolinone oxygen atom and hydrogen-bonding distance of the phenol group of T203Y.

Since the changes in fluorescence are rapid, reversible, span a large range of pH and ionic strengths,[204] and are halide specific, the YFP−H148Q mutant can be used to study halide concentrations and transport in subcellular organelles.[205]

## G. Metals

### 1. Reagentless Biosensors

Wild-type GFP has a strong affinity for Cu(II), less for Ni(II), and negligible interactions with Zn(II) and Co(II).[207] It contains 10 histidine residues, 5 of which are involved in secondary structures and are unlikely to bind metal ions. His77, His81, and His231 are all within 7.5 Å of each other in the wild-type crystal structure of GFP (1EMF) and have been proposed as a possible site for metal interaction.[207]

Since metal ions in the vicinity of a chromophore are known to quench fluorescence in a distance-dependent fashion, a metal-binding GFP mutant was designed as a potential in vivo metal ion sensor.[208] The 10C (T203Y, S54G, V68L, and S72A) GFP mutant was mutated to create two new mutants, one with a metal-binding site composed of two metal-binding residues (S147H and Q204H) and the other mutant has a tricoordinate metal-binding site (S147H, S202D and Q204H). Both the metal-binding mutants displayed fluorescence quenching at much lower metal concentrations than the 10C varient.[208]

A zinc finger domain has been inserted in place of Tyr145 in EYFP, which increased fluorescence about 1.7 times without a change in wavelength. The zinc-finger chimera only had a modest zinc affinity ($K_d$ of about 0.4mM).[64]

In section VII.C the large distance between two chromophores was mentioned as a drawback for using different colored GFPs in fluorescence resonance energy transfer (FRET). In an attempt to decrease the distance between the chromophores of the cyan (CFP) and yellow (YFP) variants of GFP in a FRET pair, CFP and YFP mutants were engineered with zinc binding sites designed to hold together a CFP/YFP dimer.[176] The FRET signal obtained from the zinc-site engineered yellow and cyan variants of GFP can be increased 8−10-fold in the presence of divalent zinc ions. A CFP and YFP FRET couple joined by a 20 amino acid linker was used as a control.[176]

### 2. Purification Aids

The affinity of GFPuv for Cu(II) and Ni(II) has been used to purify and recover GFP using immobilized metal affinity chromatography.[207] The simplest way of increasing GFP's metal affinity is to tag it with a polyhistidine. Ceramic hydroxyapatite has been used to purify both proteins and DNA. A polyhistidine-tagged GFP has been used to establish the effect of loading the hydroxyapatite with metal ions.[209] The polyhistidine-tagged GFP did not show any binding to ceramic hydroxyapatite loaded with water, and there was no observable interaction between metal-loaded ceramic hydroxyapatite and untagged GFP. However, the polyhistidine-tagged GFP showed strong binding to both Zn(II) and Fe(III).[209] A polyarginine-tagged GFP has been used to demonstrate that polyarginine-tagged fusion proteins can be immobilzed on flat surfaces, such as mica, for surface-related spectroscopic and microscopic analysis.[210]

## H. pH

Wild-type GFP and many of its mutants display pH-dependent fluorescent behavior (see section VI) and have been used to monitor pH in vivo.[84,211−215] pH-sensitive mutants with p$K_a$s ranging from 6.15 to 7.1 have been reported.[216,217] While traditional synthetic pH indicators have not been very effective at monitoring mitochondrial matrix pH, GFP-based pH indicators have successfully measured cytosolic, mitochondrial, and Golgi pH.[217] EYFP has a p$K_a$ of 7.1 and has been used as a Golgi and cytosolic pH indicator. For organelles that are more acidic than the Golgi and cytosol, EGFP is used because EYFP is nonfluorescent at these pHs.[216] ECFP is less pH sensitive than either EYFP or EGFP and is rarely used.

A series of pH-sensitive GFP mutants have been developed by structure-directed combinatorial mutagenesis; they are often known as pHluorins.[214,218] There are two types of pHluorins: ratiometric and ecliptic pHluorins. As the pH is lowered, the excitation maximum of the ratiometric pHluorins shifts from 395 to 475 nm. Therefore, the ratio of the fluorescence intensities of the two peaks can be calibrated and used to monitor the pH. In ecliptic pHluorins, the peak at 475 nm becomes nonfluorescent (eclipsed) at pHs of less than 6.0. The response to pH is reversible and occurs within 20 ms after returning to neutral pH in both the ratiometric and ecliptic pHluorins.

Fluorescence correlation spectroscopic studies of YFP showed that excitation of the anionic form of the chromophore can lead to a pathway that results in a nonprotonated dark state[118] (see section VI.G). The existence of two dark states, one protonated and the other unprotonated, may lead to incorrect calibration of GFP pH indicators; this is because it is incorrect to assume the loss of fluorescence is solely due to protonation.[118]

## I. Protein−Protein Interactions

Because any biochemical signal that changes the distance or orientation between the two fluorophores will affect the efficiency of FRET, it is a very useful technique for studying protein−protein interactions in vivo and in vitro.[5,132,150,175−177,219] Luminescence resonance energy transfer (LRET) from *Renilla* luciferase to GFP has also been used to study protein−protein interactions in living cells.[220] Two fusion proteins were expressed in CHO cells: the one linked GFP to insulin-like growth factor while the other joined *Renilla* luciferase to insulin-like growth factor binding protein. Upon addition of coelenterazine, which is required for luciferase luminescence, to cells containing the two fusion proteins, LRET occurred indicating that the GFP and luciferase chimeras were in close proximity.[220]

Chimeras of GFP linked to aequorin by a protease recognition site linker have been used to demonstrate

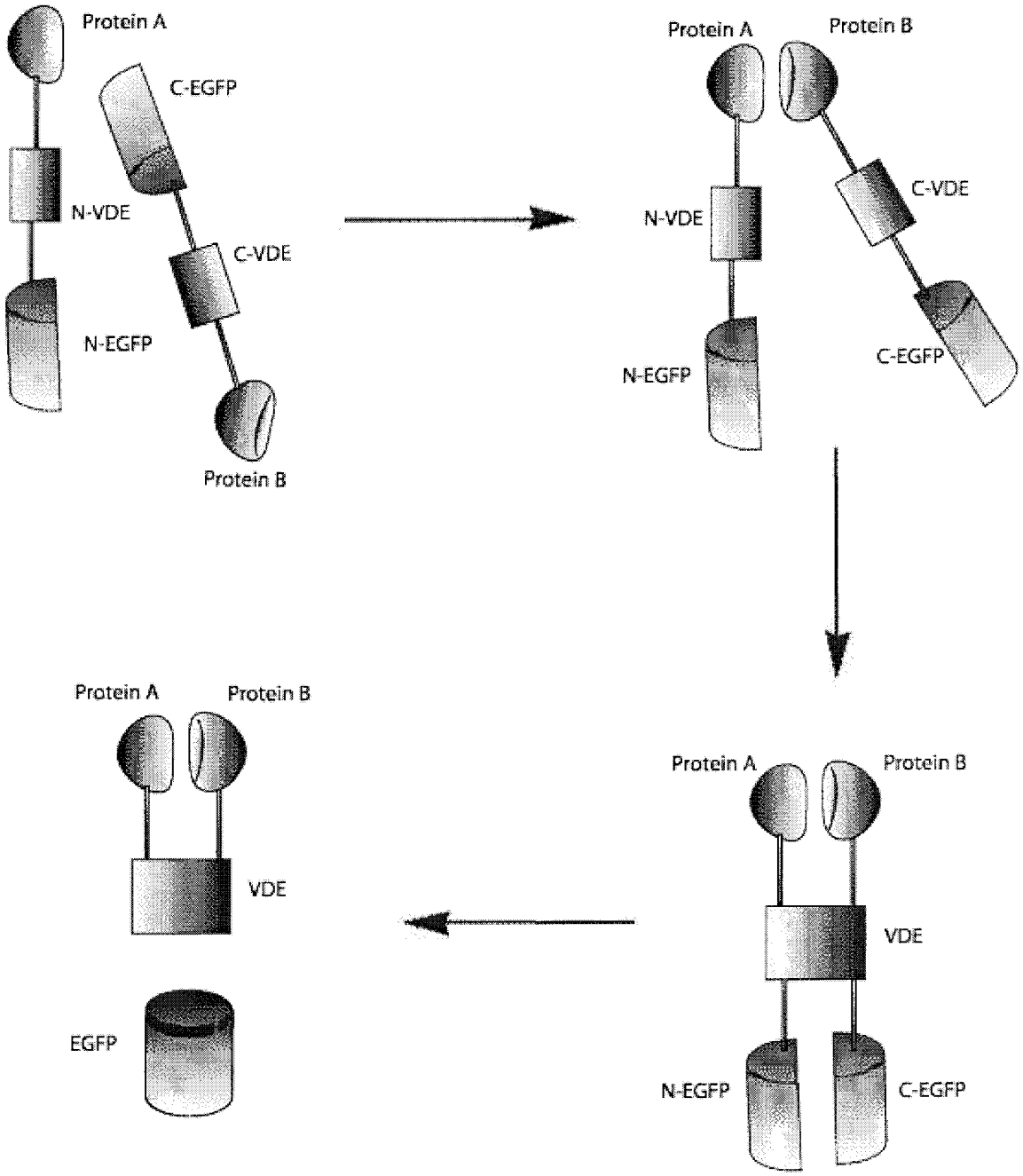


**Figure 12.** Split EGFP as a probe for protein−protein interactions. See text for full description.[225]

that chemiluminescence-resonance-energy-transfer (CRET) can be used as a homogeneous assay for proteases and perhaps other proteins.[221]

Protein−protein interactions can also be monitored by fluorescence gel retardation, fluorescence polarization assays,[222] and affinity capillary electrophoresis.[223] Fluorescence gel retardation is based on the fact that the electrophoretic mobility of a GFP−protein chimera is higher than that of a complex formed by a protein−protein interaction between the GFP−protein chimera and another protein. Some of the drawbacks of fluorescence gel retardation are that it assumes that the protein−protein interactions remain at equilibrium throughout the electrophoresis and migration though the gel. Furthermore, the conditions during electrophoresis are not always those of interest. Fluorescence polarization assays are based on the fact that a free GFP−protein chimera is likely to rotate more rapidly than a GFP−protein chimera interacting with another protein and will therefore have a lower rotational correlation time than its bound counterpart. Since fluorescence polarization assays can be performed in homogeneous solutions, in which the conditions can be controlled as desired, it is the preferred method over fluorescence gel retardation.[222,224]

A more adventurous method[225] to monitor protein−protein interactions is shown in Figure 12. To determine whether two proteins, protein A and protein B, interact, fusion proteins of each protein were created. Protein A is connected to the N terminus of one-half a protein splicing system which in turn is connected to the N terminus of one-half a EGFP. Protein B is linked to the C terminus of the other half of the

splicing system, which is linked to the C terminus of the other half of the EGFP. When proteins A and B interact, the two halves of the protein splicing systems are brought together, correct folding occurs, and the two halves of EGFP are joined by a peptide bond and released. Therefore, the amount of fluorescence, which is proportional to the number of chromophores in mature EGFPs, is proportional to the protein−protein interactions. The interaction between calmodulin and its target peptide M13 has been studied by this method.[225]

Attempts are currently underway to use GFP to characterize large numbers of protein−protein interactions in high-throughput settings.[226]

### J. Other Applications

GFP has been used as a marker for tumor cells to illuminate tumor progression and allow for detection of metastases down to the single-cell level[227−229] and as a whole-body optical imaging system in live mice.[230−232] Caution should be used when applying GFP in low oxygen conditions (hypoxia) such as those found in tumor cells.[233] Histone−GFP fusions have been designed that were sufficiently sensitive to visualize double minute chromosomes in vivo.[157] Double minute chromosomes are paired chromatin bodies found in as many as 50% of human tumors but not found in normal chromosomes. A rapid cell-based, functional assay for the screening of chemopreventive agents using GFP as a reporter gene has been developed.[234]

Using three- and four-color flow cytometry techniques, multiple variables can be evaluated at the same time. The excitation spectra of EYFP, EGFP, ECFP, and DsRed can be analyzed simultaneously by using dual-laser excitation at 458 and 568 nm and multiparameter flow cytometric methods.[235,236] The spectra of EYFP, EGFP, and ECFP can be simultaneously analyzed by single-laser excitation at 458 nm.[237]

## *VIII. GFP Analogues*

The photochemistry of green fluorescent proteins in *Renilla*, the sea pansy, has been studied and investigated for more than 30 years.[24,25] However, *Renilla* has only recently been sequenced and has not been used in many applications. The *Renilla* GFP has a 25.1% sequence identity to that of *Aequorea*[238] and a 39−48% sequence identity with Anthozoan fluorescent proteins, which are discussed in more detail later in this section. The wild-type *Renilla* and *Ptilosarcus* GFPs are more fluorescent than their *Aequorea* counterparts and are promising intercellular reporters.[238] The circular dichroism spectra and thermal melting curves of the three GFPs are all very similar, suggesting that they all adopt $\beta$-barrel conformations.[238]

Molecular biological methods were used to find GFP homologues in brightly colored corals by searching for proteins that have sequence homology with the residues in the turns between the $\beta$-sheets of GFP and the α-helix sequence that holds the chromophore in place in the center of the GFP $\beta$-can.[239] Six GFP homologues were found in the corals of the *discosoma* genus. Although they only have 26−30% sequence identity with GFP, their overall structures are remarkably similar.[240] The top (residues 82−91) and the bottom (residues 129−140) of the cans are also extremely well conserved. Both Tyr66 and Gly67, which form the chromophore in GFP, are conserved in wild-type GFP and in all six anthozoa species, as are Arg96 and Glu222. These GFP analogues have all been expressed in mammalian cell cultures.[239] The red-emitting fluorescent proteins from *discosoma* are of particular interest since they could potentially avoid autofluorescence, form new FRET partnerships, and be of use in multicolor tagging experiments. DsRed (drFP583 in the original Matz nomenclature[239]) is a red-emitting fluorescent protein from *discosoma* that is commercially available and has been studied in some detail. Residues Tyr66, Gly67, Arg96, and Glu222 in GFP correspond to Tyr67, Gly68, Arg95, and Glu215 in DsRed. It is an excellent FRET partner to YFP.

The molecular spectroscopy and dynamics of dsRed have been investigated using fluorescence correlation spectroscopy and time-correlated single-photon counting.[241] It was found that the fluorescence yield of dsRed is pH insensitive, which is unique among GFPs, and that dsRed is probably expressed as a tetramer in *E. coli*.[241] Numerous experiments[242] confirmed the spectroscopic[243] finding that DsRed is an obligate tetramer. Some denaturation has been observed under mildly acidic conditions (pH 4.0−4.8); the accompanying loss of fluorescence could be recovered by increasing the pH.[244] Biochemical, mutagenesis, and oligomerization studies of DsRed showed that it had a much higher extinction coefficient than was previously reported and was resistant to pH changes, photobleaching, and denaturing agents.[242] Furthermore, it was shown that its 583 nm emission could be shifted to longer wavelengths by selective mutations.On the basis of the high-resolution mass-spectra of lysyl endopeptidase-digested mature DsRed, a structure for the chromophore formation in DsRed has been suggested, see Figure 13, as has a mechanism for its formation.[245] The immature DsRed forms an intermediate green species by cyclization (dehydration) and oxidation (dehydrogenation) in the same way that the GFP chromophore is formed, see Figure 5. A subsequent dehydrogenation of Gln66 forms the mature red chromophore, see Figure 13. Quantum mechanical calculations have confirmed that the extended conjugation due to the acylimine accounts for the observed red shift.[245] The formation of the mature red chromophore takes from hours to days and is incomplete.[245] Point mutations such as P37S, K83R, N42H, and T217S stabilize the green immature form of DsRed, which has an absorption peaking at 480 nm.[246] Another intermediate has also been found with an absorption maximum at 408 nm; it has been suggested that the two intermediates correspond to the protonated and deprotonated forms of the chromophore, as observed in GFP, see section VI.[246]

Two groups have independently solved and reported the crystal structure of DsRed.[247,248] As predicted, see above, DsRed is found as a tetramer, the monomers consist of 11-stranded $\beta$-barrels, and the

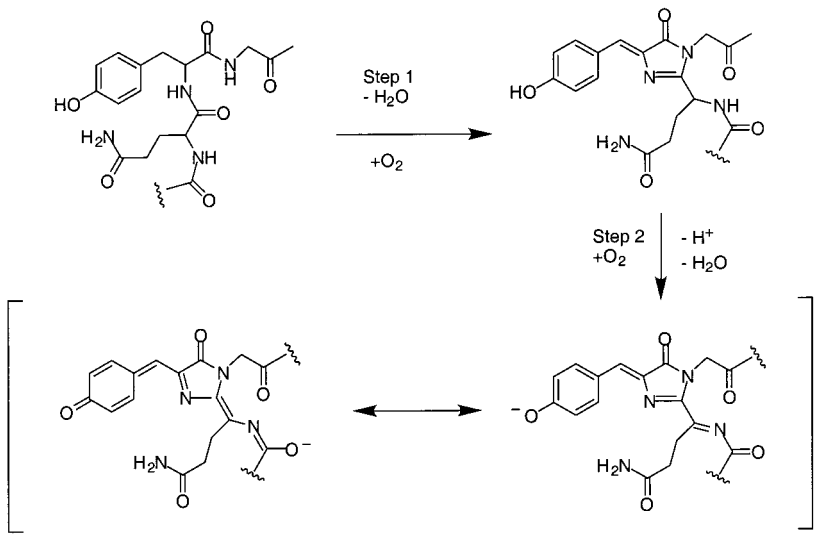


**Figure 13.** Proposed mechanism for the chromophore formation in DsRed. The immature DsRed forms an intermediate green species by cyclization (dehydration) and oxidation (dehydrogenation) in the same way that the GFP chromophore is formed, see Figure 5. A subsequent dehydrogenation of Gln66 forms the mature red chromophore with an acylimine.[245]

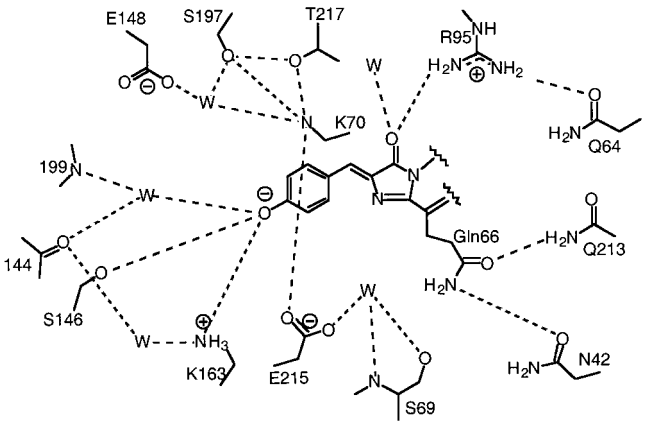


**Figure 14.** Schematic diagram of the interactions between the chromophore and its surroundings in DsRed.[248] Hydrogen bonds and salt bridges are shown as dashed lines.

chromophore has been extended by an acylimine, relative to that of GFP. An usual feature of the structure is that the amide bond preceding the acylimine has a rare cis configuration. It has been suggested[247] that isomerization of the cis peptide bond between Phe65 and Gln66 is a key step in the formation of the acylimine found in the mature DsRed and that it may be responsible for the slow maturation observed in DsRed. The monomers making up the tetramer are very similar to each other (average root-mean-square deviation of Cα atoms of 0.18 Å) and each monomer differs from GFP with an average root-mean-square deviation of Cα atoms 1.9 Å.[247] Most of the differences between DsRed and GFP are in the loop regions between the $\beta$-sheets, which are truncated in DsRed. Ten water molecules form a continuous hydrogen-bonding network that is isolated from the bulk solvent and connects the phenolic oxygens of the two closest chromophores (22 Å). The carboxy termini of the A monomer and the C monomer form a "clasp" linking the two monomers.[248]

Figure 14 shows the immediate environment around the chromophore of DsRed. There are more charged residues in the vicinity of the chromophore of DsRed than are found near the chromophore in GFP. Lys163 forms a salt bridge with the phenolic oxygen of the chromophore, indicating that the chromopohore is anionic and accounting for the relative insensitivity of DsRed fluorescence to acidification. There are two bands of charged residues, a positively charged band approximately parallel to the long axis of the chromophore, and a negatively charged band perpendicular to the long axis bisecting the chromophore.[248] A detailed mechanism for the formation of the acylimine has been proposed on the basis of the crystal structure of DsRed and on known luciferase chemistry. The mechanism[248] is shown in Figure 15.

E5 is a mutant of DsRed which changes its fluorescence from bright green to yellow, orange, and finally red over time. Because the rate of change in fluorescence is independent of protein concentration, it can be used as a fluorescent timer to monitor the activation and down-regulation of gene expression on the whole-organism scale.[249]

By using gene-shuffling techniques to generate a pool of mutants from DsRed and a new red fluorescent protein (dsFP593) and choosing a hybrid gene for subsequent random mutagenesis, a mutant was generated that has the most red-shifted emission maximum for a DsRed mutant at 616 nm.[250] By cotransfecting with cDNA encoding untagged or GFP-tagged subunits, the function of oligomeric DsRed-tagged proteins has been restored, and fluorescence was observed 12−16 h after transfection, much earlier than normal.[251]

Two green fluorescent proteins, an orange fluorescent protein, and a nonfluorescent red protein from the Mediterranean sea anemone *Anemonia sulcata* have also been isolated, tested in vivo as fusion chimeras, and characterized.[252] The red nonfluorescent protein is smaller than GFP; it has been found independently by two different groups[252,253] and presumably forms the distinctive $\beta$-barrel structure found in all GFPs by some type of multimerization process. The spectral and biophysical properties of a purple chromoprotein (asFP595) found in *Anemonia*

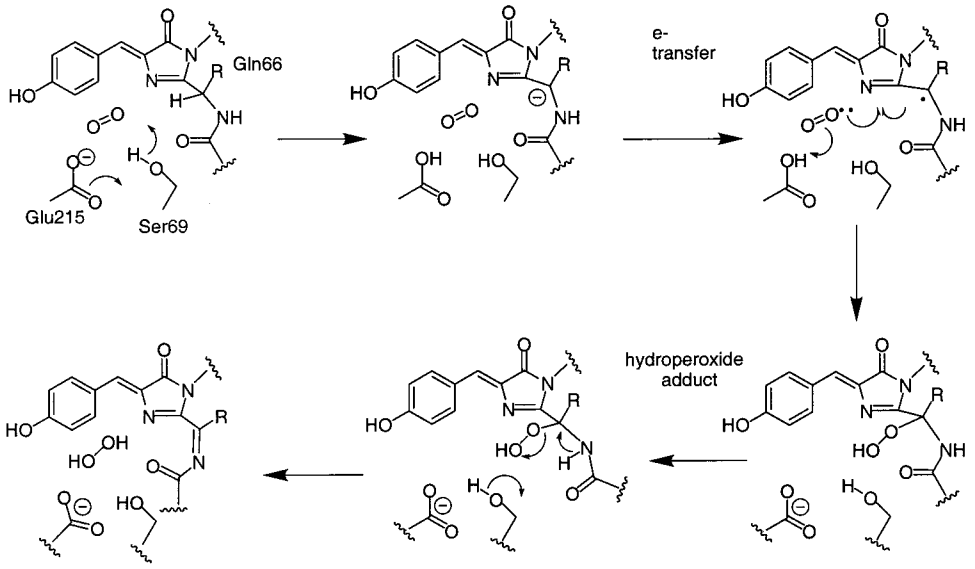


**Figure 15.** Mechanism proposed[248] for the final oxidation of dsRed.

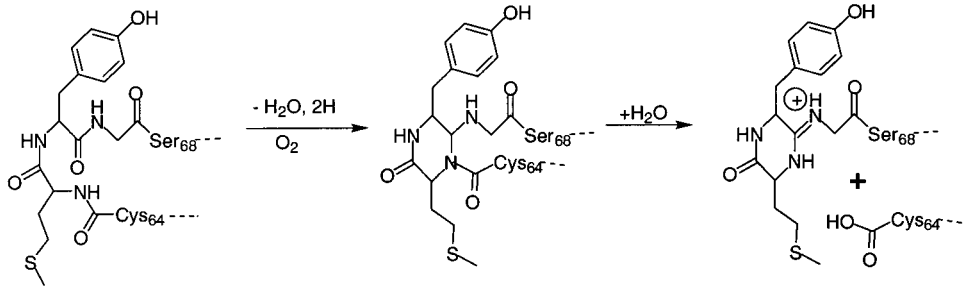


**Figure 16.** Proposed mechanism for the chromophore formation in asFP595.[254] The first two steps are a cyclization and a reduction of Tyr66. In GFP and DsRed the autocatalytic cyclization is due to the nucleophilic reaction between the amide nitrogen of Gly67 and the carbonyl carbon of residue 65, while in asFP595 the cycliztion occurs between the amide nitrogen of Met65 and the carbonyl carbon of Tyr66 forming a six-membered ring. Following cyclization the N−acylamidine bond (the former peptide bond between Cys64 and Met65) is hydrolyzed, resulting in a 8 and 20kDa fragment.[254]

*sulcata* are significantly different from GFP and DsRed.[254] At no point in its maturation does asFP595 exhibit any green fluorescence; on the basis of this observation, mass spectral studies, and biochemical assays, the mechanism shown in Figure 16 has been derived to account for chromophore formation in asFP595. The major differences between asFP595 and the other known GFP family members are that the autocatalytic cyclization forms a six-membered ring and not a five-membered ring and that cyclization is followed by hydrolyses, resulting in the splitting of the protein into 8- and 20-kDa fragments.[254] Lukyanov et al.[255] developed a method to generate far red fluorescent proteins from red nonfluorescent GFP analogues such as those found in *Heteris crispa*.

## IX. Conclusion

In less than 10 years GFP has gone from an interesting but relatively unknown protein to one of the most commonly used tools in molecular and cell biology. Despite its relatively simple structure, many questions about its folding, chromophore formation, and photophysics remain unanswered. The answers to these questions will not only help us understand GFP and its properties, but will also lead to new and improved applications. Although GFP has been used in numerous applications, there are still many applications that are waiting to benefit from GFP's fluorescence, such as the design of a reagentless zinc biosensor.

The discovery of a series of fluorescent and nonfluorescent GFP homologues in corals and sea anemones has been a very exciting development in the field. The homologues are interesting and useful, but more importantly their discovery shows that we can expect to find other GFP analogues that are stable, monomeric, nontoxic, fold, and mature rapidly at 37 °C and have the desired photophysical properties.

## X. Acknowledgment

Many thanks to all the students that have worked with me over the last 10 years. Thanks also to the Camille and Henry Dreyfus Foundation (M.Z. is Henry Dreyfus Teacher-Scholar) and to the NIH (Grant GM59108-01) and the Research Corporation for financial support.

## XI. References

(1) Chalfie, M. *Photochem. Photobiol.* **1995**, *62*, 651−656.
(2) Cubitt, A. B.; Heim, R.; Adams, S. R.; Boyd, A. E.; Gross, L. A.; Tsien, R. Y. *TIBS* **1995**, *20*, 448−455.
(3) Gerdes, H.-H.; Kaether, C. *FEBS Lett.* **1996**, *389*, 44−47.
(4) Tsien, R. *Annu. Rev. Biochem.* **1998**, *67*, 510−544.
(5) Kendall, J. M.; Badminton, M. N. *TIBTECH* **1998**, *16*, 216−224.
(6) Leffel, S. M.; Mabon, S. A.; Steward, J., C. N. *Biotechniques* **1997**, *23*, 912−918.

(7) Phillips, G. N. J. *Curr. Opin. Struct. Biol.* **1997**, *7*, 821−827.
(8) Naylor, L. H. *Biochem. Pharmacol.* **1999**, *58*, 749−757.
(9) Misteli, T.; Spector, D. L. *Nat. Biotechnol.* **1997**, *15*, 961−964.
(10) Taylor, D. L.; Woo, E. S.; Giuliano, K. A. *Curr. Opin. Biotechnol.* **2001**, *12*, 75−81.
(11) *Green Fluorescent Protein: Properties, Applications, and Protocols*; Chalfie, M., Kain, S., Eds.; Wiley-Liss: New York, 1998.
(12) *Green Fluorescent Protein*; Conn, P. M., Ed.; Academic Press: San Diego, 1999; Vol. 302.
(13) *Green Fluorescent Protein: Methods in Cell Biology*; Sullivan, K. F., Kay, S. A., Eds.; Academic Press: San Diego, 1998; Vol. 58.
(14) Matus, A. *Trends Cell Biol.* **1999**, *9*, 43−43.
(15) Matus, A. *Trends Cell Biol.* **2001**, *11*, 183.
(16) Harvey, E. N. *Bioluminescence*; Academic Press: New York, 1952.
(17) Hastings, J. W.; Morin, J. G. In *Green Fluorescent Protein*; Chalfie, M., Kain, S., Eds.; Wiley-Liss: New York, 1998.
(18) Shimomura, O. In *Green Fluorescent Protein*; Chalfie, M., Kain, S., Eds.; Wiley-Liss: New York, 1998.
(19) Prasher, D. C.; Eckenrode, V. K.; Ward, W. W.; Pendergast, F. G.; Cormier, M. J. *Gene* **1992**, *111*, 229−233.
(20) Chalfie, M.; Tu, Y.; Euskirchen, G.; Ward, W. W.; Prasher, D. C. *Science* **1994**, *263*, 802−805.
(21) Davenport, D.; Nicol, J. A. C. *Proc. R. Soc. London, Ser. B* **1955**, *144*, 399−411.
(22) Shimomura, O.; Musicki, B.; Kishi, Y. *Biochem. J.* **1988**, *251*, 405−410.
(23) Shimomura, O. *Biol. Bull.* **1995**, *189*, 1−5.
(24) Morin, J. G.; Hastings, J. W. *J. Cell Physiol.* **1971**, *77*, 313−318.
(25) Ward, W. W. *Photochem. Photobiol. Rev.* **1979**, 1−57.
(26) Morise, H.; Shimomura, O.; Johnson, F. H.; Winant, J. *Biochemistry* **1974**, *13*, 2656−2662.
(27) Head, J. F.; Inouye, S.; Teranishi, K.; Shimomura, O. *Nature* **2000**, *405*, 372−376.
(28) Shimomura, O. *FEBS Lett.* **1979**, *104*, 220−222.
(29) Cody, C. W.; Prasher, D. C.; Westler, W. M.; Pendergast, F. G.; Ward, W. W. *Biochemistry* **1993**, *32*, 1212−1218.
(30) Yang, F.; Moss, L.; Phillips, G. *Nat. Biotechnol.* **1996**, *14*, 1246−1251.
(31) Ormoe, M.; Cubitt, A. B.; Kallio, K.; Gross, L. A.; Tsien, R. Y.; Remington, S. J. *Science* **1996**, *273*, 1392−1395.
(32) Rao, B.; Kemple, M.; Pendergast, F. *Biophys. J.* **1980**, *32*, 630−632.
(33) Ward, W. W. B., S. H. *Biochemistry* **1982**, *21*, 4535−4540.
(34) Dopf, J.; Horiagon, T. M. *Gene* **1996**, *173*, 39−44.
(35) Li, X.; Zhang, G.; Ngo, N.; Zhao, X.; Kain, S.; Huang, C.-C. *J. Biol. Chem.* **1997**, *272*, 28545−28549.
(36) Brejc, K.; Sixma, T. K.; Kitts, P. A.; Kain, S. R.; Tsien, R. Y.; Ormoe, M.; Remington, S. J. *Proc. Natl. Acad. Sci.* **1997**, *94*, 2306−2311.
(37) Yang, F.; Moss, L. G.; Phillips, G. N. J. *Nat. Biotechnol.* **1996**, *14*, 1246−1251.
(38) Heim, R.; Prasher, D. C.; Tsien, R. Y. *Proc. Natl. Acad. Sci. U.S.A.* **1994**, *91*, 12501−12504.
(39) Nishiuchi, Y. I., T.; Nishio, H.; Bodi, J.; Kimura, T.; Tsuji, F. I.; Sakakiara, S. *Proc. Natl. Acad. Sci U.S.A.* **1998**, *95*, 13549−13554.
(40) Bokman, S. H.; Ward, W. W. *Biochem. Biophys. Res. Commun.* **1981**, *101*, 1372−1380.
(41) Crameri, A.; Whitehorn, E. A.; Tate, E.; Stemmer, W. P. C. *Nat. Biotechnol.* **1996**, *14*, 315−319.
(42) Reid, B. G.; Flynn, G. C. *Biochemistry* **1997**, *36*, 6786−6791.
(43) Makino, Y.; Amada, K.; Taguchi, H.; Yoshida, M. *J. Biol. Chem.* **1997**, *272*, 12468−12474.
(44) Bokman, S. H.; Ward, W. W. *Biochem. Biophys. Res. Commun.* **1981**, *101*, 1372−1380.
(45) Kane, J. F.; Hartley, D. L. *Trends Biotechnol.* **1988**, *14*, 95−101.
(46) Cormack, B. P.; Valdiva, R. H.; Falkow, S. *Gene* **1996**, *173*, 33−38.
(47) Siemering, K. R.; Globik, R.; Sever, R.; Haselhoff, J. *Curr. Biol.* **1996**, *6*, 1653−1663.
(48) Kimata, Y.; Lim, C. R.; Kohna, K. In *Green Fluorescent Protein*; Conn, P. M., Ed.; Academic Press: San Diego, 1999; Vol. 302.
(49) Delagrave, S.; Hawith, R. E.; Silva, C. M.; Yang, M. M.; Youvan, D. C. *bio/technology* **1995**, *13*, 151−154.
(50) Heim, R.; Tsien, R. *Curr. Biol.* **1996**, *6*, 178−182.
(51) Yang, T.-T.; Sinai, P.; Green, G.; Kitts, P. A.; Chen, Y.-H.; Lybarger, L.; Chervenak, R.; Patterson, G. H.; Piston, D. W.; Kain, S. R. *J. Biol.. Chem.* **1998**, *273*, 8212−8216.
(52) Cubbit, A. B.; Woolenweber, L. A.; Heim, R. *Methods Cell Biol.* **1999**, *58*, 19−30.
(53) Fukuda, H.; Arai, M.; Kuwajima, K. *Biochemistry* **2000**, *39*, 12025−12032.
(54) Sacchetti, A.; El Sewedy, T.; Nasr, A. F.; Alberti, S. *FEBS Lett.* **2001**, *492*, 151−151.
(55) Sacchetti, A.; Cappetti, V.; Marra, P.; Dell'Arciprete, R.; El Sewedy, T.; Crescenzi, C.; Alberti, S. *J. Cell. Biochem.* **2001**, 117−128.
(56) Sakikawa, C.; Taguchi, H.; Makino, Y.; Yoshida, M. *J. Biol. Chem.* **1999**, 21251−21256.
(57) Weber-Ban, E. U.; Reid, B. G.; Miranker, A. D.; Horwich, A. L. *Nature* **1999**, *401*, 90−93.
(58) Battistutta, R.; Negro, A.; Zanotti, G. *Proteins: Struct., Funct., Genet.* **2000**, *41*, 429−437.
(59) Palm, G. J.; Zdanov, A.; Gaitanaris, G. A.; Stauber, R.; Pavlakis, G. N.; Wlodawer, A. *Nat. Struct. Biol.* **1997**, *4*, 361−365.
(60) Branchini, B. R.; Nemser, A. R.; Zimmer, M. *J. Am. Chem. Soc.* **1998**, *120*, 1−6.
(61) Merkel, J. S.; Regan, L. *J. Biol. Chem.* **2000**, *275*, 29200−29206.
(62) This reference was deleted on revision.
(63) Helms, V.; Straatsma, T. P.; McCammon, J. A. *J. Phys. Chem. B* **1999**, *103*, 3263−3269.
(64) Baird, G. S.; Zacharias, D. A.; Tsien, R. Y. *Proc. Natl. Acad. Sci. U.S.A.* **1999**, *96*, 11241−11246.
(65) Ghosh, I.; Hamilton, A. D.; Regan, L. *J. Am. Chem. Soc.* **2000**, *122*, 5658−5659.
(66) Nagai, T.; Sawano, A.; Park, E. S.; Miyawaki, A. *Proc. Natl. Acad. Sci. U.S.A.* **2001**, *98*, 3197−3202.
(67) Abedi, M. R.; Caponigro, G.; Kamb, A. *Nucleic Acid Res.* **1998**, *26*, 623−630.
(68) Chiang, C. F.; Okou, D. T.; Griffin, T. B.; Verret, C. R.; Williams, M. N. V. *Arch. Biochem. Biophys.* **2001**, *394*, 229−235.
(69) Schwede, T. F.; Retey, J.; Schulz, G. E. *Biochemistry* **1999**, *38*, 5355−5361.
(70) Donnelly, M.; Fedeles, F.; Wirstam, M.; Siegbahn, P. E. M.; Zimmer, M. *J. Am. Chem. Soc.* **2001**, *123*, 4679−4686.
(71) Heim, R.; Cubitt, A.; Tsien, R. Y. *Nature* **1995**, *373*, 663−664.
(72) Branchini, B. R.; Lusins, J. O.; Zimmer, M. *J. Biomol. Struct. Dyn.* **1997**, *14*, 441−448.
(73) Zimmer, M.; Branchini, B. R.; Lusins, J. O. In *Bioluminescence and chemiluminescence*; Hastings, J. W., Kricka, L. J., Stanley, P. E., Eds.; John Wiley: Chichester, England, 1996; Vol. 9.
(74) Remington, S. J. In *Bioluminescence and Chemiluminescence, Pt. C*; *Methods in Enzymology*; Academic Press Inc.: San Diego, 2000; Vol. 305.
(75) Siegbahn, P. E. M.; Wirstam, M.; Zimmer, M. *Int. J. Quantum Chem.* **2001**, *81*, 169−186.
(76) Creemers, T. M. H.; Lock, A. J.; Subramaniam, V.; Jovin, T. M.; Volker, S. *Nat. Struct. Biol.* **1999**, *6*, 557−560.
(77) Niwa, H.; Inouye, S.; Hirano, T.; Matsuno, T.; Kojima, M.; Kubota, M.; Ohashi, M.; Tsuji, F. I. *Proc. Natl. Acad. Sci. U.S.A.* **1996**, 13617−13622.
(78) Ward, W. W.; Prentice, H. J.; Roth, A. F.; Cody, C. W.; Reeves, S. C. *Photochem. Photobiol.* **1982**, *35*, 803−808.
(79) Lossau, H.; Kummer, A.; Heinecke, R.; Poellinger-Dammer, F.; Kompa, C.; Bieser, G.; Jonsson, T.; Silva, C. M.; Yang, M. M.; Youvan, D. C.; Michel-Beyerle, M. E. *Chem. Phys.* **1996**, *213*, 1−16.
(80) Kummer, A.; Wiehler, J.; Rehaber, H.; Kompa, C.; Steipe, B.; Michel-Beyerle, M. *J. Phys. Chem.* **2000**, *104*, 4791−4798.
(81) Chattoraj, M.; King, B. A.; Bublitz, G. U.; Boxer, S. G. *Proc. Natl. Acad. Sci. U.S.A.* **1996**, *93*, 8362−8367.
(82) Yazal, J. E.; Pendergast, F. G.; Shaw, D. E.; Pang, Y.-P. *J. Am. Chem. Soc.* **2000**, *122*, 11411−11416.
(83) Elowitz, M. B.; Surette, M. G.; Wolf, P.-E.; Stock, J.; Leibler, S. *Curr. Biol.* **1997**, *7*, 809−812.
(84) Wachter, R. M.; King, B. A.; Heim, R.; Kallio, K.; Tsien, R. Y.; Boxer, S. G.; Remington, S. J. *Biochemistry* **1997**, *36*, 9759−9765.
(85) Bublitz, G.; King, B.; Boxer, S. *J. Am. Chem. Soc.* **1998**, *120*, 9370−9371.
(86) Elsliger, M. A.; Wachter, R. M.; Hanson, G. T.; Kallio, K.; Remington, S. J. *Biochemistry* **1999**, *38*, 5296−5301.
(87) Scharnagl, C.; RauppKossmann, R.; Fischer, S. F. *Biophys. J.* **1999**, *77*, 1839−1857.
(88) Warren, A.; Zimmer, M. *J. Mol. Graphics Modell.* **2001**, *19*, 297−303.
(89) Seebacher, C.; Deeg, F.; Brauchle, C.; Wiehler, J.; Steipe, B. *J. Phys. Chem.* **1999**, *103*, 7728−7732.
(90) Jung, G.; Zumbusch, A.; Brauchle, C. *J. Phys. Chem.* **2000**, *104*.
(91) Ward, W. W.; Cody, C. W.; Hart, R. C.; Cormier, M. J. *Photochem. Photobiol.* **1980**, *31*, 611−615.
(92) Shimomura, O. *FEBS Lett.* **1979**, *104*, 220−222.
(93) McCapra, F.; Razavi, Z.; Neary, A. P. *J. Chem. Soc., Chem. Commun.* **1988**, 790−791.
(94) You, Y. J.; He, Y. K.; Borrows, P. E.; Forrest, S. R.; Petasis, N. A.; Thompson, M. E. *Adv. Mater.* **2000**, *12*, 1678+.
(95) Kummer, A. D.; Kompa, Lossau, H.; Poellinger-Dammer, F.; Michel-Beyerle, M.-E.; Silva, C. M.; Bylina, E. J.; Coleman, W. J.; Yang, M. M.; Youvan, D. C. *Chem. Phys.* **1998**, *237*, 183−193.
(96) Voityuk, A. A.; Michel-Beyerle, M.-E.; Roesch, N. *Chem. Phys. Lett.* **1998**, *296*, 269−276.
(97) Chen, M. C.; Lambert, C. R.; Urgitis, J. D.; Zimmer, M. *Chem. Phys.* **2001**, *270*, 157−164.

(98) Webber, N. M.; Litvinenko, K. L.; Meech, S. R. *J. Phys. Chem. B* **2001**, *105*, 8036−8039.
(99) Weber, W.; Helms, V.; McCammon, J.; Langhoff, P. *Proc. Natl. Acad. Sci. U.S.A.* **1999**, *96*, 6177−6182.
(100) Striker, G.; Subramaniam, V.; Seidel, C. A. M.; Volkmer, A. *J. Phys. Chem. B* **1999**, *103*, 8612−8617.
(101) van Thor, J.; Pierik, A.; Nugteren-Roodzant, I.; Xie, A.; Hellingwerf, K. *Biochemistry* **1998**, *37*, 16915−16921.
(102) Yoo, H. Y.; Boatz, J. A.; Helms, V.; McCammon, J. A.; Langhoff, P. W. *J. Phys. Chem. B* **2001**, *105*, 2850−2857.
(103) Kummer, A. D.; Wiehler, J.; Rehaber, H.; Kompa, C.; Steipe, B.; MichelBeyerle, M. E. *J. Phys. Chem. B* **2000**, *104*, 4791−4798.
(104) Voityuk, A. A.; Michel-Beyerle, M.-E.; Roesch, N. *Chem. Phys. Lett.* **1997**, *272*, 162−167.
(105) Voityuk, A. A.; Michel-Beyerele, M.-E.; Roesch, N. *Chem. Phys.* **1998**, *231*, 13−25.
(106) Bell, A. F.; He, X.; Wachter, R. M.; Tonge, P. J. *Biochemistry* **2000**, *39*, 4423−4431.
(107) Schellenberg, P.; Johnson, E.; Esposito, A. P.; Reid, P. J.; Parson, W. W. *J. Phys. Chem. B* **2001**, *105*, 5316−5322.
(108) Dickson, R. M.; Cubitt, A. B.; Tsien, R. Y.; Moerner, W. E. *Nature* **1997**, *388*, 355−358.
(109) Peterman, E. J. G.; Brasselet, S.; Moerner, W. E. *J. Phys. Chem. A* **1999**, *103*, 10553−10560.
(110) Garcia-Parajo, M. F.; Segers-Nolten, G. M. J.; Veerman, J.-A.; Greeve, J.; Hulst, N. F. v. *Proc. Nat. Acad. Sci. U.S.A.* **2000**, *97*, 7237−7242.
(111) Pierce, D. W.; HomBooher, N.; Vale, R. D. *Nature* **1997**, *388*, 338−338.
(112) Pierce, D. W.; Vale, R. D. *Methods Cell. Biol.* **1998**, *58*, 49−73.
(113) Jung, G.; Brauchle, C.; Zumbusch, A. *J. Chem. Phys.* **2001**, *114*, 3149−3156.
(114) Harms, G. S.; Cognet, L.; Lommerse, P. H. M.; Blab, G. A.; Schmidt, T. *Biophys. J.* **2001**, *80*, 2396−2408.
(115) Cinelli, R. A. G.; Pellegrini, V.; Ferrari, A.; Faraci, P.; Nifosi, R.; Tyagi, M.; Giacca, M.; Beltram, F. *Appl. Phys. Lett.* **2001**, *79*, 3353−3355.
(116) Wachter, R. M.; Elsiger, M. A.; Kallio, K.; Hanson, G. T.; Remington, S. J. *Structure* **1998**, *6*, 1267−1277.
(117) Griesbeck, O.; Baird, G. S.; Campbell, R. E.; Zacharias, D. A.; Tsien, R. Y. *J. Biol. Chem.* **2001**, *276*, 29188−29194.
(118) Schwille, P.; Kummer, S.; Heikal, A. A.; Moerner, W. E.; Webb, W. W. *Proc. Nat. Acad. Sci. U.S.A.* **2000**, *97*, 151−156.
(119) Ehrig, T.; O'Kane, D. J.; Pendergast, F. G. *FEBS Lett.* **1995**, *367*, 163−166.
(120) Palm, G. J.; Wlodawer, A. *Methods Enzymol.* **1999**, *302*, 378−394.
(121) Helms, V.; Winstead, C.; Langhoff, P. W. *J. Mol. Struct. (THEOCHEM)* **2000**, *506*, 179−189.
(122) Hanazono, Y.; Yu, J. M.; Dunbar, C. E.; Emmons, R. V. B. *Hum. Gene Ther.* **1997**, *8*, 1313−1319.
(123) Liu, H. S.; Jan, M. S.; Chou, C. K.; Chen, P. H.; Ke, N. J. *Biochem. Biophys. Res. Commun.* **1999**, *260*, 712−717.
(124) Wahlfors, J.; Loimas, S.; Pasanen, T.; Hakkarainen, T. *Histochem. Cell Biol.* **2001**, *115*, 59−65.
(125) Ehrmann, M. A.; Scheyhing, C. H.; Vogel, R. F. *Lett. Appl. Microbiol.* **2001**, *32*, 230−234.
(126) Chiu, W.-l.; Niwa, Y.; Zeng, W.; Hirano, T.; Kobayashi, H.; Sheen, J. *Curr. Biol.* **1996**, *6*, 325−330.
(127) Davis, S. J. V., R. D. *Plant Mol. Biol.* **1998**, *36*, 521−528.
(128) Cormack, B. P.; Bertram, G.; Egerton, M.; Gow, N. A.; Falcow, S. *Microbiology* **1997**, *143*, 303−311.
(129) Lorang, J. M.; Tuori, R. P.; Martinez, J. P.; Sawyer, T. L.; Redman, R. S.; Rollins, J. A.; Wolpert, T. J.; Johnson, K. B.; Rodriguez, R. J.; Dickman, M. B.; Ciuffetti, L. M. *Appl. Environ. Microbiol.* **2001**, *67*, 1987−1994.
(130) Kirkpatrick, S. M.; Naik, R. R.; Stone, M. O. *J. Phys. Chem. B* **2001**, *105*, 2867−2873.
(131) Lippincott-Schwartz, J.; Snapp, E.; Kenworthy, A. *Nat. Rev. Mol. Cell Biol.* **2001**, *2*, 444−456.
(132) Bastiaens, P. I. H.; Pepperkok, R. *Trends Biochem. Sci.* **2000**, *25*, 631−637.
(133) Billinton, N.; Knight, A. W. *Anal. Biochem.* **2001**, *291*, 175−197.
(134) Hanson, M. R.; Kohler, R. H. *J. Exp. Bot.* **2001**, *52*, 529−539.
(135) Stewart, C. N. *Plant Cell Rep.* **2001**, *20*, 376−382.
(136) Phillips, G. J. *FEMS Microbiol. Lett.* **2001**, *204*, 9−18.
(137) Zernicka-Goetz, M.; Pines, J. *Methods* **2001**, *24*, 55−60.
(138) Burd, C. G. In *Applications of Chimeric Genes and Hybrid Proteins, Pt. B; Methods in Enzymology*; Academic Press Inc.: San Diego, 2000; Vol. 327.
(139) Ikawa, M.; Yamada, S.; Nakanishi, T.; Okabe, M. In *Current Topics in Developmental Biology*; Academic Press Inc.: San Diego, 1999; Vol. 44.
(140) Shinbrot, E.; Spencer, C.; Natale, V.; Kain, S. R. In *Applications of Chimeric Genes and Hybrid Proteins Pt. B; Methods in Enzymology*; Academic Press Inc.: San Diego, 2000; Vol. 327.
(141) Wouters, F. S.; Verveer, P. J.; Bastiaens, P. I. H. *Trends Cell Biol.* **2001**, *11*, 203−211.
(142) Belmont, A. S. *Trends Cell Biol.* **2001**, *11*, 250−257.
(143) Toomre, D.; Manstein, D. J. *Trends Cell Biol.* **2001**, *11*, 298−303.
(144) Chan, A. W. S.; Chong, K. Y.; Martinovich, C.; Simerly, C.; Schatten, G. *Science* **2001**, *291*, 309−312.
(145) *Eduardo Kac: Telepresence, Biotelematics and Transgenic Art.; GFP Bunny*; Dobrila, P. T., Kostic, A., Eds.; Kibla: Maribor, Slovenia, 2000.
(146) Okabe, M.; Ikawa, M.; Kominami, K.; Nakanishi, T.; Nishimune, Y. *FEBS Lett.* **1997**, *407*, 313−319.
(147) Mercuri, A.; Sacchetti, A.; De Benedetti, L.; Schiva, T.; Alberti, S. *Plant Sci.* **2001**, *161*, 961−968.
(148) Gory, L.; Montel, M. C.; Zagorec, M. *FEMS Microbiol. Lett.* **2001**, *194*, 127−133.
(149) Dandie, C. E.; Thomas, S. M.; McClure, N. C. *Lett. Appl. Microbiol.* **2001**, *32*, 26−30.
(150) Tsien, R. Y. *Annu. Rev. Biochem.* **1998**, *67*, 509−544.
(151) Zhu, H. Y.; Yamada, H.; Jiang, Y. M.; Yamada, M.; Nishiyama, Y. *Arch. Virol.* **1999**, *144*, 1923−1935.
(152) McLean, A. J.; Bevan, N.; Rees, S.; Milligan, G. *Mol. Pharmacol.* **1999**, *56*, 1182−1191.
(153) Haraguchi, T.; Ding, D. Q.; Yamamoto, A.; Kaneda, T.; Koujin, T.; Hiraoka, Y. *Cell Struct. Funct.* **1999**, *24*, 291−298.
(154) Wymer, C. L.; Fernandez-Abalos, J. M.; Doonan, J. H. *Planta* **2001**, *212*, 692−695.
(155) Ward, B. M.; Moss, B. *J. Virology* **2001**, *75*, 4802−4813.
(156) Martinez-Torres, A.; Miledi, R. *Proc. Nat. Acad. Sci. U.S.A.* **2001**, *98*, 1947−1951.
(157) Kanda, T.; Sullivan, K. F.; Wahl, G. M. *Curr. Biol.* **1998**, *8*, 377−385.
(158) Siegel, M. S.; Isacoff, E. Y. *Neuron* **1997**, *19*, 735−741.
(159) Biondi, R. M.; Baehler, P. J.; Reymond, C. D.; Vernon, M. *Nucleic Acid Res.* **1998**, *26*, 4946−4952.
(160) Hink, M. A.; Griep, R. A.; Borst, J. W.; vanHoek, A.; Eppink, M. H. M.; Schots, A.; Visser, A. J. W. G. *J. Biol. Chem.* **2000**, *275*, 17556−17560.
(161) Prescott, M.; Nowakowski, S.; Nagley, P.; Devendish, R. *Anal. Biochem.* **1999**, *273*, 305−307.
(162) Dabrowski, S.; Brillowska-Dabrowska, A.; Kur, J. *Biotechniques* **2000**, *29*, 800−806.
(163) Kotarsky, K.; Owman, C.; Olde, B. *Anal. Biochem.* **2001**, *288*, 209−215.
(164) Miller, S.; Kennedy, D.; Thomson, J.; Han, F.; Smith, R.; Ing, N.; Piedrahita, J.; Busbee, D. *Toxicol. Sci.* **2000**, *55*, 69−77.
(165) Sun, Y.; Wong, M. D.; Rosen, B. P. *J. Biol. Chem.* **2001**, *276*, 14955−14960.
(166) Zhao, H.; Ivic, L.; Otaki, J. M.; Hashimoto, M.; Mikoshiba, K.; Firestein, S. *Science* **1998**, *279*, 237−242.
(167) Josenhans, C.; Friedrich, S.; Suerbaum, S. *FEMS Microbiology* **1998**, *161*, 263−273.
(168) Lemaire-Vieille, C.; Schulze, T.; Podevin-Dimster, V.; Follet, J.; Bailly, Y.; Blanquet-Grossard, F.; Decavel, J. P.; Heinen, E.; Cesbron, J. Y. *Proc. Natl. Acad. Sci. U.S.A.* **2000**, *97*, 5422−5427.
(169) Miller, W. G.; Brandl, M. T.; Quinones, B.; Lindow, S. E. *Appl. Environ. Microbiol.* **2001**, *67*, 1308−1317.
(170) Dumas, B.; Centis, S.; Sarrazin, N.; Esquerre-Tugaye, M. T. *Appl. Environ. Microbiol.* **1999**, *65*, 1769−1771.
(171) Jacobi, C. A.; Roggenkamp, A.; Rakin, A.; Zumbihl, R.; Leitritz, L.; Heesemann, J. *Mol. Microbiol.* **1998**, *30*, 865−882.
(172) Jung, S.; Aliberti, J.; Graemmel, P.; Sunshine, M. J.; Kreutzberg, G. W.; Sher, A.; Littman, D. R. *Mol. Cell. Biol.* **2000**, *20*, 4106−4114.
(173) Sexton, A. C.; Howlett, B. J. *Physiol. Mol. Plant Pathol.* **2001**, *58*, 13−21.
(174) Li, X.; Zhao, X.; Fang, Y.; Jiang, X.; Duong, T.; Fan, C.; Huang, C.-C.; Kain, S. *J. Biol. Chem.* **1998**, *273*, 34970−34975.
(175) Bastiaens, P. I. H.; Jovin, T. M. In *Cell biology: A laboratory handbook*; Celis, J. E., Ed.; Academic Press: 1998.
(176) Jensen, K. K.; Martini, L.; Schwartz, T. W. *Biochemistry* **2001**, *40*, 938−945.
(177) Pozzan, T. *Nature* **1997**, *388*, 834−835.
(178) Pollok, B. A.; Heim, R. *Trends Cell Biol.* **1999**, *9*, 57−60.
(179) Miyawaki, A.; Llopis, J.; Heim, R.; McCaffrey, J. M.; Adams, J. A.; Ikura, M.; Tsien, R. Y. *Nature* **1997**, *388*, 882−887.
(180) Miyawaki, A.; Griesbeck, O.; Heim, R.; Tsien, R. Y. *Proc. Nat. Acad. Science U.S.A.* **1999**, *96*, 2135−2140.
(181) Day, R. N. *Mol. Endocrinol.* **1998**, *12*, 1410−1419.
(182) Mahajanm, N. P.; Linder, K.; Berry, G.; Gordon, G. W.; Heim, R.; Herman, B. *Nat. Biotechnol.* **1998**, *16*, 547−552.
(183) Xu, X.; Gerad, A. L.; Huang, B. C.; Anderson, D. C.; Payan, D. G.; Luo, Y. *Nucleic Acids Res.* **1998**, *26*, 2034−2035.
(184) Suzuki, Y.; Yasunaga, T.; Ohkura, R.; Wakabayaschi, T.; Sutoh, K. *Nature* **1998**, *396*, 380−383.
(185) Harpur, A. G.; Wouters, F. S.; Bastiaens, P. I. H. *Nat. Biotechnol.* **2001**, *19*, 167−169.
(186) Griffin, B. A.; Adams, S.; Tsien, R. *Science* **1998**, *281*, 269−272.

(187) Creemers, T. M. H.; Lock, A. J.; Subramaniam, V.; Jovin, T. M.; Volker, S. *Proc. Nat. Acad. Sci. U.S.A.* **2000**, *97*, 2974−2978.
(188) Pearce, L. L.; Gandley, R. E.; Han, W.; Wasserloos, K.; Stitt, M.; Kanai, A. J.; McLaughlin, M. K.; Pitt, B. R.; Levitan, E. S. *Proc. Natl. Acad. Sci. U.S.A.* **2000**, *97*, 477−482.
(189) Persechini, A.; Lynch, J. A.; Romoser, V. A. *Cell Calcium* **1997**, *22*, 209−216.
(190) Mahajan, N. P.; HarrisonShostak, D. C.; Michaux, J.; Herman, B. *Chem. Biol.* **1999**, *6*, 401−409.
(191) Nagai, Y.; Miyazaki, M.; Aoki, R.; Zama, T.; Inouye, S.; Hirose, K.; Iino, M.; Hagiwara, M. *Nat. Biotechnol.* **2000**, *18*, 313−316.
(192) White, J.; Stelzer, E. *Trends Cell Biol.* **1999**, *9*, 61−65.
(193) Reits, E. A. J.; Neefjes, J. J. *Nat. Cell Biol.* **2001**, *3*, E145−E147.
(194) Bardeen, C. J.; Yakovlev, V. V.; Squier, J. A.; Wilson, K. R. *J. Am. Chem. Soc.* **1998**, 13023−13027.
(195) Allen, G. J.; Kwak, J. M.; Chu, S. P.; Llopis, J.; Tsien, R. Y.; Harper, J. F.; Schroeder, J. I. *Plant J.* **1999**, *19*, 735−747.
(196) Emmanouilidou, E.; Teschemacher, A. G.; Pouli, E. A.; Nicholls, L. I.; Seward, E. P.; Rutter, G. A. *Curr. Biol.* **1999**, *9*, 915−918.
(197) Kerr, R.; Lev-Ram, V.; Baird, G.; Vincent, P.; Tsien, R. Y.; Schafer, W. R. *Neuron* **2000**, *26*, 583−594.
(198) Yu, R.; Hinkle, P. M. *J. Biol. Chem.* **2000**, *275*, 23648−23653.
(199) Jaconi, M.; Bony, C.; Richards, S. M.; Terzic, A.; Arnaudeau, S.; Vassort, G.; Puceat, M. *Mol. Biol. Cell* **2000**, *11*, 1845−1858.
(200) Remington, S. J. In *Bioluminescence and Chemiluminescence, Pt C*; Academic Press Inc.: San Diego, 2000; Vol. 305.
(201) Mizuno, H.; Sawano, A.; Eli, P.; Hama, H.; Miyawaki, A. *Biochemistry* **2001**, *40*, 2502−2510.
(202) Baubet, V.; Le Mouellic, H.; Campbell, A. K.; Lucas-Meunier, E.; Fossier, P.; Brulet, P. *Proc. Natl. Acad. Sci. U.S.A.* **2000**, *97*, 7260−7265.
(203) Nakai, J.; Ohkura, M.; Imoto, K. *Nat. Biotechnol.* **2001**, *19*, 137−141.
(204) Wachter, R. M.; Remington, S. J. *Curr. Biol.* **1999**, *9*, R628−R629.
(205) Jayaraman, S.; Haggie, P.; Wachter, R. M.; Remington, S. J.; Verkman, A. S. *J. Biol. Chem.* **2000**, *275*, 6047−6050.
(206) Wachter, R. M.; Yarbrough, D.; Kallio, K.; Remington, S. J. *J. Mol. Biol.* **2000**, *301*, 157−171.
(207) Li, Y.; Arawal, A.; Sakon, J.; Beitle, R. R. *J. Chromatogr. A* **2001**, *909*, 183−190.
(208) Richmond, T.; Takahashi, T.; Shimkhada, R.; Bernsdorf, J. *Biochem. Biophys. Res. Commun.* **2000**, *268*, 462−465.
(209) Nordstrom, T.; Senkas, A.; Eriksson, S.; Poentynen, N.; Nordstrom, E.; Lindqvist, C. *J. Biotechnol.* **1999**, *69*, 125−133.
(210) Nock, S.; Spudich, J. A.; Wagner, P. *FEBS Lett.* **1997**, *414*, 233−238.
(211) Takahashi, A.; Zhang, Y. P.; Centonze, V. E.; Herman, B. *Biotechniques* **2001**, *30*, 804−812.
(212) Robey, R. B.; Ruiz, O.; Santos, A. V. P.; Ma, J. F.; Kear, F.; Wang, L. J.; Li, C. J.; Bernardo, A. A.; Arruda, J. A. L. *Biochemistry* **1998**, *37*, 9894−9901.
(213) Elsliger, M. A.; Wachter, R. M.; Hanson, G. T.; Kallio, K.; Remington, S. J. *Biochem. Usa* **1999**, *38*, 5296−5301.
(214) Yuste, R.; Miller, R. B.; Holthoff, K.; Zhang, S.; Miesenboeck, G. In *Cell Biology and Physiology*; Thorner, J., Emr, S. D., Abelson, J. N., Eds.; Academic Press: San Diego, 2000; Vol. 327.
(215) Moseyko, N.; Feldman, L. J. *Plant Cell Environ.* **2001**, *24*, 557−563.
(216) Llopis, J.; McCaffery, J. M.; Miyawaki, A.; Farquhar, M. G.; Tsien, R. Y. *Proc. Natl. Acad. Sci. U.S.A.* **1998**, *95*, 6803−6808.
(217) Takahashi, A.; Zhang, Y. P.; Centonze, V. E.; Herman, B. *Biotechniques* **2001**, *30*, 804−+.
(218) Miesenboeck, G.; Angelis, D. A. D.; Rothman, J. E. *Nature* **1998**, *394*, 192.
(219) Truong, K.; Ikura, M. *Curr. Opin. Struct. Biol.* **2001**, *11*, 573−578.
(220) Wang, Y.; Wang, G.; O'Kane, D. J.; Szalay, A. A. *Mol. Gen. Genet.* **2001**, *264*, 578−587.
(221) Waud, J. P.; Fajardo, A. B.; Sudhaharan, T.; Trimby, A. R.; Jeffery, J.; Jones, A.; Campbell, A. K. *Biochem. J.* **2001**, *357*, 687−697.
(222) Park, S. H.; Raines, R. T. In *Applications of Chimeric Genes and Hybrid Proteins, Pt. C; Methods in Enzymology*; Academic Press Inc.: San Diego, 2000; Vol. 328.
(223) Kiessig, S.; Reissmann, J.; Rascher, C.; Kullertz, G.; Fischer, A.; Thunecke, F. *Electrophoresis* **2001**, *22*, 1428−1435.
(224) Park, S.-H.; Raines, R. T. *Protein Science* **1997**, *6*, 2344−2349.
(225) Ozawa, T.; Nogami, S.; Sato, M.; Ohya, Y.; Umezawa, Y. *Anal. Chem.* **2000**, *72*, 5151−5157.
(226) Endoh, H.; Walhout, A. J. M.; Vidal, M. In *Applications of Chimeric Genes and Hybrid Proteins, Pt. C; Methods in Enzymology*; Academic Press Inc.: San Diego, 2000; Vol. 328.
(227) Chishima, T.; Miyagi, Y.; Wang, X.; Baranov, E.; Tan, Y.; Shimada, H.; Moossa, A. R.; Hoffman, R. M. *Clin. Exp. Metastasis* **1997**, *15*, 547−552.
(228) Chishima, T.; Miyagi, Y.; Wang, X.; Yamaoka, H.; Shimada, H.; Moossa, A. R.; Hoffman, R. M. *Cancer Res.* **1997**, *57*, 2042−2047.
(229) Hoffman, R. M. *Biotechniques* **2001**, *30*, 1024−1026.
(230) Yang, M.; Baranov, E.; Li, X. M.; Wang, J. W.; Jiang, P.; Li, L.; Moossa, A. R.; Penman, S.; Hoffman, R. M. *Proc. Natl. Acad. Sci. U.S.A.* **2001**, *98*, 2616−2621.
(231) Rashidi, B.; Yang, M.; Jiang, P.; Baranov, E.; An, Z. L.; Wang, X.; Moossa, A. R.; Hoffman, R. M. *Clin. Exp. Metastasis* **2000**, *18*, 57−60.
(232) Yang, M.; Baranov, E.; Moossa, A. R.; Penman, S.; Hoffman, R. M. *Proc. Natl. Acad. Sci. U.S.A.* **2000**, *97*, 12278−12282.
(233) Coralli, C.; Cemazar, M.; Kanthou, C.; Tozer, G. M.; Dachs, G. U. *Cancer Res.* **2001**, *61*, 4784−4790.
(234) Zhu, M.; Fahl, W. E. *Anal. Biochem.* **2000**, *287*, 210−217.
(235) Hawley, T. S.; Telford, W. G.; Ramezani, A.; Hawley, R. G. *Biotechniques* **2001**, *30*, 1028−1034.
(236) Hawley, T. S.; Telford, W. G.; Hawley, R. G. *Stem Cells* **2001**, *19*, 118−124.
(237) Beavis, A.; Kalejta, R. *Cytometry* **1999**, *37*, 51−59.
(238) Peelle, B.; Gururaja, T. L.; Payan, D. G.; Anderson, D. C. *J. Protein Chem.* **2001**, *20*, 507−519.
(239) Matz, M. V.; Fradkov, A. F.; Labas, Y. A.; Savitisky, A. P.; Zaraisky, A. G.; Markelov, M. L.; Lukyanov, S. A. *Nat. Biotechnol.* **1999**, *17*, 969−973.
(240) Tsien, R. Y. *Nat. Biotechnol.* **1999**, *17*, 956−957.
(241) Heikal, A. A.; Hess, S. T.; Baird, G. S.; Tsien, R. Y.; Webb, W. W. *Proc. Natl. Acad. Sci. U.S.A.* **2000**, *97*, 14831−14831.
(242) Baird, G. S.; Zacharias, D. A.; Tsien, R. Y. *Proc. Natl. Acad. Sci. U.S.A.* **2000**, *97*, 11984−11989.
(243) Heikal, A. A.; Hess, S. T.; Baird, G. S.; Tsien, R. Y.; Webb, W. W. *Proc. Natl. Acad. Sci. U.S.A.* **2000**, *97*, 11996−12001.
(244) Vrzheshch, P. V.; Akovbian, N. A.; Varfolomeyev, S. D.; Verkhusha, V. V. *FEBS Lett.* **2000**, *487*, 203−208.
(245) Gross, L. A.; Baird, G. S.; Hoffman, R. C.; Baldridge, K. K.; Tsien, R. Y. *Proc. Natl. Acad. Sci. U.S.A.* **2000**, *97*, 11990−11995.
(246) Wiehler, J.; von Hummel, J.; Steipe, B. *FEBS Lett.* **2001**, *487*, 384−389.
(247) Wall, M. A.; Socolich, M.; Ranganathan, R. *Nat. Struct. Biol.* **2000**, *7*, 1133−1138.
(248) Yarbrough, D.; Wachter, R. M.; Kallio, K.; Matz, M. V.; Remington, S. J. *Proc. Natl. Acad. Sci. U.S.A.* **2001**, *98*, 462−467.
(249) Terskikh, A.; Fradkov, A.; Ermakova, G.; Zaraisky, A.; Tan, P.; Kajava, A. V.; Zhao, X. N.; Lukyanov, S.; Matz, M.; Kim, S.; Weissman, I.; Siebert, P. *Science* **2000**, *290*, 1585−1588.
(250) Fradkov, A. F.; Chen, Y.; Ding, L.; Barsova, E. V.; Matz, M. V.; Lukyanov, S. A. *FEBS Lett.* **2000**, *479*, 127−130.
(251) Lauf, U.; Lopez, P.; Falk, M. M. *FEBS Lett.* **2001**, *498*, 11−15.
(252) Wiedenmann, J.; Elke, C.; Spindler, K. D.; Funke, W. *Proc. Natl. Acad. Sci. U.S.A.* **2000**, *97*, 14091−14096.
(253) Lukyanov, K. A.; Fradkov, A. F.; Gurskaya, N. G.; Matz, M. V.; Labas, Y. A.; Savitsky, A. P.; Markelov, M. L.; Zaraisky, A. G.; Zhao, X. N.; Fang, Y.; Tan, W. Y.; Lukyanov, S. A. *J. Biol. Chem.* **2000**, *275*, 25879−25882.
(254) Martynov, V. I.; Savitsky, A. P.; Martynova, N. Y.; Savitsky, P. A.; Lukyanov, K. A.; Lukyanov, S. A. *J. Biol. Chem.* **2001**, *276*, 21012−21016.
(255) Gurskaya, N. G.; Fradkov, A. F.; Terskikh, A.; Matz, M. V.; Labas, Y. A.; Martynov, V. I.; Yanushevich, Y. G.; Lukyanov, K. A.; Lukyanov, S. A. *FEBS Lett.* **2001**, *507*, 16−20.
(256) Berman, H. M.; Westbrook, J.; Feng, Z.; Gilliland, G.; Bhat, T. N.; Weissig, H.; Shindyalov, I. N.; Bourne, P. E. *Nucleic Acids Res.* **2000**, *28*, 235−242.
(257) Ostergaard, H.; Henriksen, A.; Hansen, F. G.; Winther, J. R. *EMBO J.* **2001**, *20*, 5853−5862.
(258) Griesbeck, O.; Baird, G. S.; Campbell, R. E. Tsien R. Y. Manuscript in preparation.

CR010142R